A Markov chain-based approach for assessing respiratory infection risk in a multi-zone office building

Zhen, Qi; Zhang, Anxiao; Bokel, Regina; Zheng, Yue; Li, Jing; Du, Yiming; Zhang, Qi

DOI
10.1016/j.jobe.2024.109328

Publication date
2024

Document Version
Final published version

Published in
Journal of Building Engineering

Citation (APA)
Zhen, Q., Zhang, A., Bokel, R., Zheng, Y., Li, J., Du, Y., & Zhang, Q. (2024). A Markov chain-based approach for assessing respiratory infection risk in a multi-zone office building. *Journal of Building Engineering*, *90*, Article 109328. https://doi.org/10.1016/j.jobe.2024.109328

Journal of Building Engineering 90 (2024) 109328

Contents lists available at ScienceDirect

Journal of Building Engineering

journal homepage: www.elsevier.com/locate/jobe

A Markov chain-based approach for assessing respiratory infection risk in a multi-zone office building

Qi Zhen [a,b], Anxiao Zhang [a,b,*], Regina Bokel [c], Yue Zheng [a], Jing Li [d], Yiming Du [a], Qi Zhang [a]

[a] School of Architecture, Tianjin University, Tianjin, China
[b] Key Laboratory of Ecology and Energy Saving Study of Dense Habitat, Ministry of Education, China
[c] Faculty of Architecture and the Built Environment, Delft University of Technology, Delft, the Netherlands
[d] School of Public Health, Tianjin Medical University, Tianjin, China

ARTICLE INFO

Keywords:
Space design
Occupant behavior
Respiratory infection risk assessment
Office building
Markov chain

ABSTRACT

Most respiratory infectious disease transmission events occur in indoor environments, and examining the infection risk in different types of multi-zone buildings is critical to the safe reopening and use of public buildings. Appropriate space design influences occupant behavior and virus spread, thereby aiding in mitigating indoor infection risk. This study aims to quickly evaluate the multi-route infection risk in multi-zone buildings with relatively stable occupant populations, and to quantify the effectiveness of spatial interventions at different levels. A Markov chain-based approach was proposed to characterize occupants' time-activity trajectories with low time cost and relatively high accuracy. Four transmission routes are considered, especially for the fine-grained characterization of close contact. A real university office building was selected as a case study to quantitatively evaluate the effects of three non-pharmacological interventions including spatial layout, ventilation, and occupant behavioral control. Results showed that short-range airborne transmission dominated, and optimized combination spatial design interventions reduced the indoor infection risk by up to 10 %. Zone layout intervention was the most effective, with the division of the open-plan office area into three subzones, reducing the risk by 9.6 %, which was superior to the intervention of maintaining a one-meter interpersonal distance. Followed by the furniture layout, without changing the seating capacity and without desktop baffles, the L-shaped table layout worked better reducing the risk by 2.78 %. This study can help architects and managers better understand the risk of indoor transmission in multizone buildings from a spatial design perspective, to select appropriate interventions to reduce the risk.

Nomenclature

A_e	Area of eyes (cm^2)
A_m	Area of mouth (cm^2)
A_n	Area of nose (cm^2)
A_f	Area of a finger (cm^2)
A_{hs}	Contact area between hand and surface (cm^2)

* Corresponding author. School of Architecture, Tianjin University, No. 92 Weijin Street, Nankai District, Tianjin, 300072, China.
E-mail address: zhanganxiao9012@gmail.com (A. Zhang).

https://doi.org/10.1016/j.jobe.2024.109328
Received 21 December 2023; Received in revised form 10 April 2024; Accepted 13 April 2024
Available online 21 April 2024

A_{hf}	Contact area between hand and membrane (cm^2)
AE	Aspiration efficiency
C	Airborne droplet concentration (droplets/m^3)
D_{LD}	Large droplet exposure dose (RNA copies)
D_{LR}	Long-range airborne exposure dose (RNA copies)
D_F	Fomite exposure dose (RNA copies)
D_{SR}	Short-range airborne exposure dose (RNA copies)
D_h	Viruses on hands (RNA copies)
DE	Deposition efficiency
d_0	Droplets' initial diameters (μm)
d_h	Diameter of head (cm)
d_m	Diameter of mouth (cm)
E_{LD}	Instantaneous large droplet exposure dose (RNA copies)
E_{LR}	Instantaneous long-range airborne exposure dose (RNA copies)
E_F	Instantaneous fomite exposure dose (RNA copies)
E_{SR}	Instantaneous short-range airborne exposure dose (RNA copies)
k	Infectious dose (PFU)
k_c	Constant
n_0	Droplets' initial numbers
q_a	Viruses' decay rate in the air (percent/s)
q_{ma}	Mask filtration efficiency for aerosols
q_{md}	Mask filtration efficiency for droplets
q_{in}	Inhalation rate (m^3/min)
q_s	Viruses' decay rate on steel (percent/s)
q_p	Viruses' decay rate on plastic (percent/s)
TE_{hf}	Transfer efficiency between hands and facial membranes
TE_{sh}	Transfer efficiency between hands and surfaces
v_0	Initial velocity of droplets exhaled (m/s)
v_{in}	Inhalation velocity (m/s)
ρ_v	Virus density in droplets (RNA copies/ml)
γ_{hf}	Frequency of hand touching facial membranes (touches/min)

1. Introduction

Since the onset of the 21st century, there has been a notable increase in the emergence of various new types of respiratory infectious diseases (RIDs), significantly impacting global health, society, and the economy. Over 90 % of outbreaks occur in indoor environments, particularly in densely populated public spaces, where close contact among individuals is deemed the primary cause of transmission [1]. Occupants' behaviors can be divided into context-related behaviors and contagion-related behaviors [2]. The contagion-related behaviors directly affect occupant exposure level, e.g., breathing patterns [3], close contact with others [4], mask use [5,6], and touching environmental surfaces [7]The context-related behaviors refer to the various activities that occupants engage in the current environment, such as walking, meeting and printing, which is the premise of contagion-related behaviors.

The type and layout of a space play a key role in shaping occupants' spatiotemporal behaviors [8], including movement trajectories [9] and close-contact interactions [10]. Additionally, factors like spatial configuration, surface materials [11], as well as temperature and humidity levels [12], influence the distribution and activity of indoor viruses. Several studies have examined the impact of spatial design on individual infection risk, aiming to ensure safe distances by optimizing the placement of spatial obstacles. Contardo et al. [13] examined the layout of tables and chairs in a restaurant to increase capacity and still maintain safe distances. Zhang et al. [10] modeled the effect of supermarket layout design on prevalence risk. Cui et al. [9] explored how the size and location of obstacles affect indoor pedestrian flow. These studies provide insights into the effectiveness of spatial interventions, but only discuss localized furniture or facility design, ignoring the effects of overall spatial layout on close contact.

Public buildings can be classified into two categories based on the behavioral characteristics of the occupants [10]. One type of buildings characterized by frequent movement of occupants, such as supermarkets, airports etc. People have relatively short overall dwell time in such spaces, and their positions change continuously over time. The other with relatively fixed occupants, such as offices, hospitalization units etc., where occupants have designated positions that they occupy for longer periods, along with other intermittent random activities. RID risk assessment in public spaces where pedestrians move frequently is usually studied through Pedestrian Dynamics Models (PDMs) such as social force models and agent-based models [14].

Exposure risk assessment methods for public spaces with relatively fixed occupants are usually based on Computational Fluid Dynamics (CFD) simulations. The CFD method is often used to assess airborne transmission risks because it can help to track in detail the diffusion process of released droplets where the virus attaches and the distribution of indoor airflow [15,16]. However, CFD simulation is usually limited to the study of airborne particles in a single small space because it requires significant computational

resources and time costs to capture the details of airflow in indoor spaces. Moreover, this method is only applicable for situations where the occupant is stationary or moves briefly in a straight line [17]. In real-world scenarios, many office buildings comprise multiple interconnected rooms, with occupants moving between them sporadically, for instance, to visit restrooms. This dynamic situation poses challenges for CFD simulations as accurately defining boundary conditions becomes complex and computationally demanding. Some studies have attempted to calculate airborne risk in multi-zone buildings using CFD methods [18,19], but still idealize them based on the building layout, i.e., the building is simplified into a set of zones, where temperature and pollutant concentrations in each zone are considered well-mixed, and inter-zone interactions are discussed through pressure variations.

PDMs, while can be applied to multi-zone office-like environments, still face computational burdens when used to complexly capture prolonged human motion, such as an eight-hour workday. Furthermore, studies have demonstrated that maintaining an interpersonal distance of 2.0 m reduces the exposure risk for susceptible individuals to just one-thousandth of the risk observed when the distance is 0.4 m [20]. In contrast, in risk assessment models based on pedestrian dynamics, the spread of viral particles was characterized by dividing the space into cells, and the particles within each cell was assumed to be uniformly distributed. The variation of particle concentrations with distance in close encounters is therefore not described with sufficient precision.

Examining the infection risk of RIDs in different types of multi-zone buildings is vital for the safe reopening and utilization of public buildings during and after the pandemic. It is essential to evaluate building protection at the architectural level based on actual spatial layout and occupant behaviors, rather than just room-level evaluations. This study delves into typical behaviors in buildings with relatively fixed occupant, using multi-zone office buildings as a case study. Occupant activities in office buildings usually follow a certain pattern, such as arrival at work and lunch, with occasional random movement events, such as trips to the water fountain to fetch water and trips to the restroom. Particularly in open-plan offices, occupants share the same space for long periods of time, and close contact often occurs during the performance of various activities [21]. While previous studies based on pedestrian dynamics have focused on portraying occupant behaviors such as movement and queuing, while neglecting the fine-grained representation of proximity contact. Ensuring computational efficiency and accurately characterizing human behavior in multi-zone office environments and linking it to viral transmission models is a challenge.

This study aims to rapidly evaluate the risk of RID spreading through multiple transmission routes in multi-zone buildings with relatively stable occupant populations, and to compare the effectiveness of spatial interventions at different levels with common measures. A Markov chain (MC)-based approach was proposed to assess the respiratory infection risk in multi-zone buildings with relatively stable occupant profiles. MC is a discrete stochastic process model that can be used to model the time-dependent and time-independent behavior of occupants with low time cost. This method enables the characterization of occupants' spatiotemporal activity trajectories by incorporating real building information and occupant behavior data, thus facilitating the calculation of exposure dose and overall infection risk associated with four transmission routes (large droplet route, short-range airborne route, long-range airborne route, and fomite route). Specifically, the study focuses on close contact during people movement, achieving a precision of 0.1 m in calculating large droplet and close airborne transmission, marking a 5-fold enhancement in accuracy compared to the grid-based description in previous models based on pedestrian dynamics. In addition, this study proposes the zonal cumulative virus exposure dose (ZCVE) as a metric for building zoning risk assessment. A real university office building was selected as a case study to validate and demonstrate the model as well as to evaluate the effects of three non-pharmacological interventions including spatial layout, ventilation, and occupant behavioral control.

2. Methods

2.1. Simulation framework

This study proposed a Markov model chain model to integrate building information, occupant behavior, and multi-route virus transmission to assess the combined infection risk of office buildings. As shown in Fig. 1, the model chain contains of four parts. First,

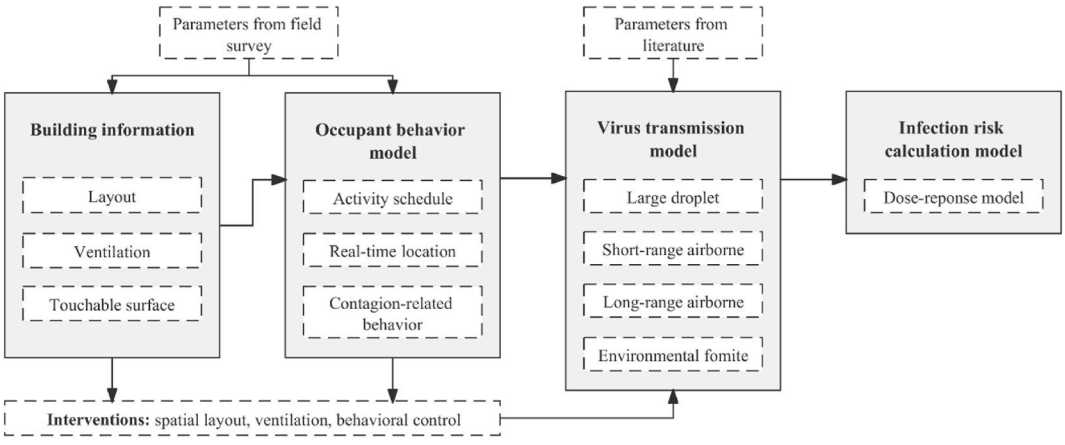

Fig. 1. Model chain of infection risk assessment in office buildings.

building information was collected. Then an occupant model was made using occupants' real-time locations and contagion-related behaviors based on the surveyed activity information. Next, a virus transmission model was made based on the exposure doses from different exposure routes. Finally, a comprehensive infection risk assessment was performed. MATLAB R2021b was used for the integration of the sub-models.

Indoor virus exposure was modeled at three levels: the individual level, the zone level, and the building level (Fig. 2). Exposure at individual level was defined as close contact within a certain social distance (e.g., 2 m), including face-to-face contact, when large droplets and short-range airborne routes may occur (Fig. 2 (a)). Note that when $\theta_2 > \theta_1/2$, no short-range exposure was assumed. Zone-level exposure referred to susceptible individuals being in the same room as the infected, with the potential for long-range airborne and fomite routes (Fig. 2 (b)). Building-level exposure in turn was more complex, involving the movement of occupants across multiple zones (Fig. 2 (c)). Both individual-level and zone-level exposures need to be considered for each time step.

The simulation procedure and computational flow were depicted in Fig. 3. Floor plans could be drawn and imported by external building modeling tools, such as AutoCAD, following certain rules. The building information was expressed through points and lines, and layers were used to distinguish obstacles, doors, zones, etc. Note that the building geometry modeled through AutoCAD cannot be directly imported into MATLAB for simulation but requires necessary preprocessing steps. First, the created building model needs to be exported as a.dxf file and imported into ArcMap software for vectorized processing and adding a coordinate system. Then the file in.shp format, based on "point" and "line", can be exported, and read with MATLAB's built-in *shaperead* command.

2.2. Building information inputs

The spatial environment affects not only the behavior of occupants but also the spread and survival of viruses [2]. Therefore, the inputs of building information included detailed building floor plan layout, ventilation patterns, location distribution of occupants, location of touchable surfaces and their materials. The details were demonstrated in the case study in Section 3.1.

Since multi-zone buildings contain a variety of functional spaces as well as different area ratios, it is necessary to study the spatial partitioning to calculate the exposure dose for each zone. In real scenarios, occupants are not evenly distributed in the space [22], for example, with the same area per capita, the interpersonal distance in a conference room may be smaller than that in an open office area. Therefore, the use of per capita square meters to define the zone may be a little biased. Interpersonal interaction is important when calculating the risk of indoor respiratory infections and is also an important basis for the division of zones in this paper. Studies [23,24] have shown that spatial layout, visibility, and accessibility levels are important factors affecting human interaction. When there are obvious obstacles in the space that affect the visual field, the space should be divided into two zones.

In addition, in current research on airborne and fomite transmission risk calculations, the division of areas is usually based on rooms or functions. Guo et al. [19] considered a room as a zone; Shrestha et al. [18] regard the area connected by adjacent rooms with

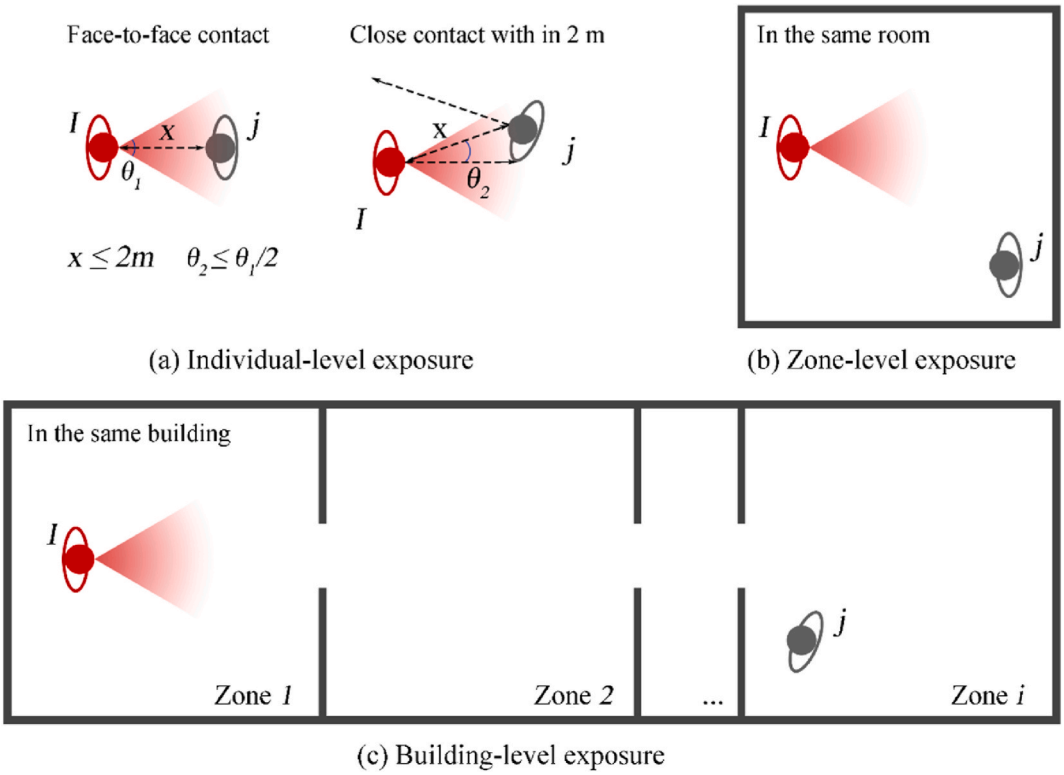

Fig. 2. Exposure levels in office buildings.

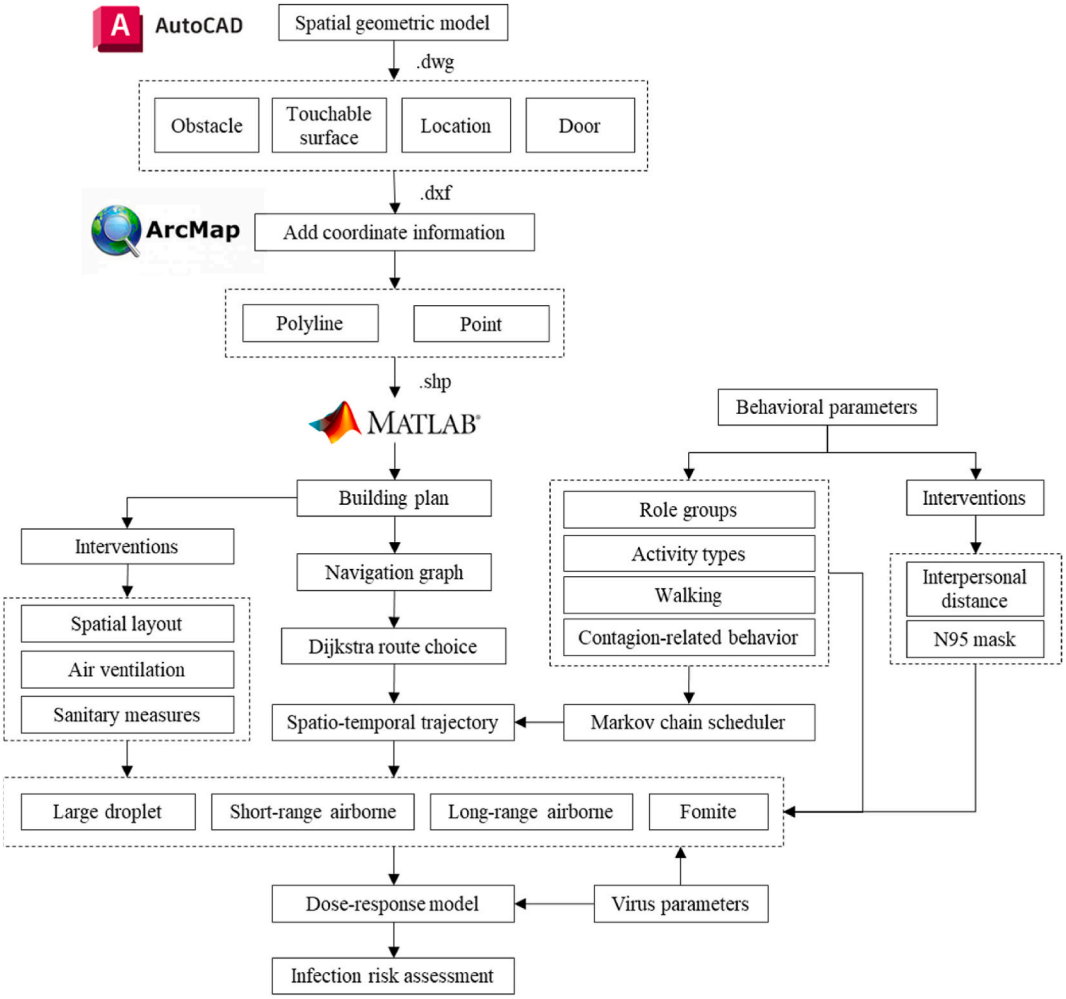

Fig. 3. Simulation procedure and computational flow.

the same function as a zone to simplify calculations; Xiao et al. [25] divided an irregular room into several zones according to function and pressure differences.

In this article, first considering long-range airborne transmission, a zone should not be larger than a room. In addition, the movement of individuals and their interactions are affected by spatial layout and visual field [23], parameters in the spatial syntax are used to qualify the division of "Zone" (Fig. 4). First, a zone should be a Convex Space, which is defined by Hillier et al. [26] as "a space in which all points are visible to each other". This concept comes from convex polygon [9], which means that if any one of the edges of a polygon is extended indefinitely in both directions to become a straight line, all other edges are on the same side of the line. Secondly, the visual area of the occupant at any point in the Zone should cover the entire space in which a person may walk in the Zone, and

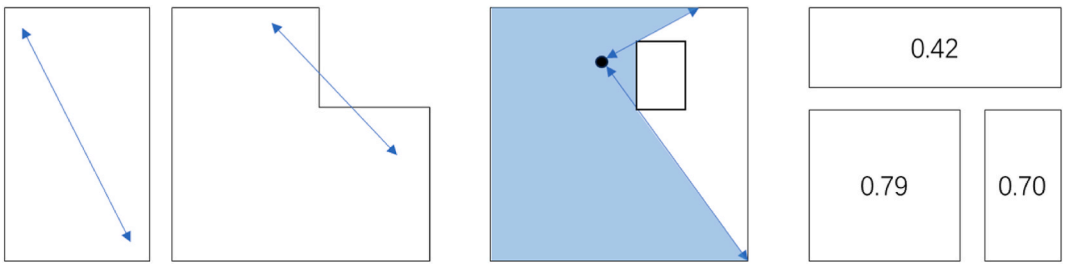

Fig. 4. The boundary conditions of a "zone".

obstacle should not exceed the height of a person's eyes when standing. Finally, the compactness of the Zone needs to be examined. Spatial accessibility consists of spatial dimensions and shapes, and in the absence of significant differences in dimensions, spatial shapes may be more important, e.g., people are more likely to move in long, narrow spaces and stay in square spaces. The compactness C_{om} can be used to characterize this feature of space and is calculated by the following formula.

$$C_{om} = \frac{{P_e}^2}{4 \times \pi \times A_r} \tag{1}$$

where P_e is the perimeter of the shape and A_r is the area of the shape. As the shape gets closer to a circle, its value gets closer to 1. In this paper, the compactness value of a Zone is defined to be not less than 0.6.

2.3. Occupant behavior model

Occupant's context-related behaviors include the occupant's activities and his/her movement between the locations of the two activities [2]. During this process, contagion-related behaviors may occur, including respiratory activities, close contact with others, touching environmental surfaces, hand washing, etc. First, the occupants' activity types in an office building were identified based on their roles and appropriate methods were selected to schedule them. Then, the temporal activity trajectory of the occupant was generated through activity scheduling and localization, which led to the real-time location of the occupant. Finally, the occurrence of contagion-related behaviors was determined based on the occupant's activity localization and the distance between the occupants.

2.3.1. Markov chain-based activity scheduler

As shown in Table 1, individual activities of occupants in office buildings were categorized into time-dependent and time-independent activities based on their relevance to time. Time-dependent activities generally have fixed start and end times and are of the highest priority. These activities are basic schedules for occupants that vary with their roles, e.g., janitors will arrive earlier than employees and managers. Time-independent activities generally occur within the time frame allowed for time-dependent activities and are of lower priority. These activities may be repeated, and their duration is generally regular. For example, printing may take 2 min but the time and number of times it occurs throughout the day is variable. In addition, working takes up most of the occupant's time. After all the above activities are scheduled, the rest of the time is spent on working. To make the simulation results close to reality, the occupant behavior model was driven by survey data.

The activity-based MC models of Shelat et al. [27] and Wang et al. [28] were referred to for the activity scheduling model. Based on the survey data (questionnaires, observations, sensors, etc.), time-dependent activities were arranged using an event scheduler. Gaps in the schedule were filled by time-independent activities and they were considered as states of an MC. First-order discrete-time MC was adopted. The time-independent activity was considered as a set of discrete random variables with Markovian properties $X = \{X_n: n > 0\}$. The set S consisting of all possible values of X_n is the state space of X. Due to the memoryless nature of MC, the current state j depends only on the state i of the previous time step, and the transfer probability p_{ij} denotes the probability of transferring from state i to j. The two-dimensional matrix P consisting of the transfer probabilities between all states in the state space S is the transfer probability matrix. All elements in P are nonnegative and the sum of the elements in each row is 1.

$$p_{ij} = P(X_{n+1} = j | X_n = i) = P(X_{n+1} = j | X_n = i, X_{n-1} = i_{n-1}, \cdots, X_0 = i_0), i, j \in S \tag{2}$$

$$P = \begin{bmatrix} p_{11} & p_{12} & \cdots & p_{1n} \\ p_{21} & p_{22} & \cdots & p_{2n} \\ \vdots & \vdots & \ddots & \vdots \\ p_{n1} & p_{n2} & \cdots & p_{nn} \end{bmatrix}, \forall p_{ij} \geq 0, \sum_{j=1}^{n} p_{ij} = 1 \tag{3}$$

An active state transfer matrix is generated for each occupant. The MC representing the activity state of an individual is irreducible and ergodic with a unique stationary probability distribution $\pi = \{\pi_n : n > 0\}$ and the sum of π is 1. The MC's dwell time in state i is T_i and the average dwell time $E(T_i) = 1/(1 - p_{ii})$. When the average duration and interval of each activity were used as inputs to the model, then the transfer probability matrix can be set up through a linear constraint matrix least squares problem [27]. The system of linear equations and the optimization problem for the n-state MC are shown in Eq. (3), respectively. The function *lsqlin* in the MATLAB software was chosen to solve the problem. One of the time-independent activities is randomly selected as the initial state, and then each subsequent time-step is simulated based on the generated transfer matrix P.

Table 1
Activity types of occupants in office building.

Activity Type	Start Time	Period	Location	Examples
Time-dependent activities	Fixed	Random	Fixed	Arrival, departure, lunch, meeting
Time-independent activities	Random	Regular	Semi-fixed	Going to the toilet, printing

$$M=\begin{bmatrix} 0 & 0 & 0 & \cdots & 0 & \cdots & 0 & 0 & 0 & \cdots & 0 \\ \pi_1 & 0 & 0 & \cdots & 0 & \cdots & \pi_n & 0 & 0 & \cdots & 0 \\ 0 & \pi_1 & 0 & \cdots & 0 & \cdots & 0 & \pi_n & 0 & \cdots & 0 \\ \vdots & \vdots & \vdots & \ddots & \vdots & \vdots & \vdots & \vdots & \vdots & \ddots & \vdots \\ 0 & 0 & \cdots & \cdots & \pi_1 & \cdots & 0 & 0 & \cdots & \cdots & \pi_n \\ 1 & 1 & 1 & \cdots & 1 & \cdots & 0 & 0 & 0 & \cdots & 0 \\ 0 & 0 & 0 & \cdots & 0 & \cdots & 0 & 0 & 0 & \cdots & 0 \\ 0 & 0 & 0 & \cdots & 0 & \cdots & 0 & 0 & 0 & \cdots & 0 \\ \vdots & \vdots & \vdots & \ddots & \vdots & \vdots & \vdots & \vdots & \vdots & \ddots & \vdots \\ 0 & 0 & 0 & \cdots & 0 & \cdots & 1 & 1 & 1 & \cdots & 1 \end{bmatrix}_{2n\times n(n-1)} \quad N=\begin{bmatrix} \pi_1(1-p_{11}) \\ \pi_2(1-p_{22}) \\ \vdots \\ \pi_n(1-p_{nn}) \\ 1-p_{11} \\ 1-p_{22} \\ \vdots \\ 1-p_{nn} \end{bmatrix}_{2n\times 1}$$

$$x=\begin{bmatrix} p_{12} \\ \vdots \\ p_{1n} \\ p_{21} \\ \vdots \\ p_{2n} \\ \vdots \\ p_{n1} \\ \vdots \\ p_{nn-1} \end{bmatrix}_{n(n-1)\times 1} \qquad min\ \|Mx-N\|_2, x>0 \tag{4}$$

2.3.2. Real-time locations

A position assignment model is used to generate the positions corresponding to each activity. Time-dependent activities have fixed locations, e.g., arrival and departure locations are building entrances. The location associated with time-independent activities is semi-fixed. Since multiple activities may occur in the same zone, in this paper the semi-fixed locations were considered as sub-zones, each corresponding to an activity. If there were multiple locations in a subzone, the availability of these locations was checked by a location scheduling program. If occupants find more than one available location, they choose the one closest to their current location. Moreover, the time to move from one activity location to another was considered.

2.3.3. Route choice

After scheduling the time and location of the activities, the path of movement between the two activity locations needs to be considered. Studies have shown that pedestrians' route choice is generally affected by individual characteristics (gender, age, vision, etc.) and environmental factors (building layout, signs, congestion, etc.) [23]. Mobility motivation and familiarity with the environment are the basic factors that affect route choice [23]. Motivation indicates people's moving purpose. People with a clear purpose are more inclined to choose the shortest route [29], such as commuters in office buildings. People who do not have a clear purpose are more likely to choose a route with more visual attractions [30], such as visitors in a museum. In multi-zone office buildings with relatively fixed personnel, occupants are generally familiar with the environment and each move is accompanied by a clear purpose (e.g. go to a meeting, go to the toilet and print), so the shortest path algorithm can be used for route search and choice [31].

Since the activity locations were finite, and the start and destination of the occupants were known, Dijkstra's algorithm was used to solve the shortest path problem [32]. The building plan was considered as an oriented graph and the locations corresponding to each activity were considered as nodes on it. Furniture and facilities were obstacles that interfered with occupants' walking, so several additional nodes were set up around them to allow pedestrians to bypass them. In addition, the process of moving between individuals was independent of each other.

2.3.4. Contagion-related behavior

As shown in Table 2, infection-related behaviors include persistent behaviors, activity-based behaviors, and location-based behaviors. Persistent behaviors including breathing, talking, and coughing, occurred at a fixed frequency and in an unrestricted location.

Table 2
Contagion-related behavior types.

Behavior Type	Frequency	Period	Location	Examples
Persistent behaviors	Regular	Regular	–	Respiration
Activity-based behaviors	Random	Regular	Fixed	Touching surface, hand washing
Location-based behaviors	Random	Random	Random	Close contact

Activity-based behaviors occurred in conjunction with activities, including touching environmental surfaces and hand washing. For example, occupants would touch the printer buttons when printing materials. Location-based behaviors referred to close contact behaviors and were related to the relative position of two individuals. Based on the real-time position of the occupant generated by the model, the distance between two individuals at any given moment can be calculated to determine whether close contact occurs.

2.4. Virus transmission model

2.4.1. Large droplet route

When a susceptible individual is within 2.0 m of an infected individual, large droplets and short-range airborne transmission may occur, due to droplet deposition and inhalation respectively [4]. Distributions of droplet initial diameters and numbers during coughing and talking were derived from the experimental results of Chao et al. [33]. The cough frequency of infected individuals was assumed to be 19 % per minute [34]. The exposure dose by large droplet route $D_{LD}(t)$ at time t can be calculated by the following equations [35,36]:

$$D_{LD}(t) = \int_0^t E_{LD}dt \tag{5}$$

$$E_{LD}(x) = \sum_{i=1}^{16} n_{xi}^{D} \bullet V_i \bullet DE_i \bullet \rho_v \bullet (1 - q_{md}) \tag{6}$$

$$DE_i = \frac{St_i^{\,2}}{\left(St_i^h + 0.25\right)^2} \tag{7}$$

where $E_{LD}(x)$ is the exposure dose at distance x from the infected individual; i is the droplet group; n_{xi}^{D} is the number of droplets deposited on the facial membranes at distance x; V_i is the volume of single droplet; DE_i is the deposition efficiency; ρ_v is the virus density in droplets; $q_{md} = (A_n + A_m)/(A_e + A_n + A_m)$ is the filtration efficiency of the mask for droplets. It prevented deposition in the nose (A_n) and mouth (A_m), but not in that of the eyes (A_e). DE_i is the deposition efficiency [37]. It is related to the Stokes number of the droplets (St_i^h), which is a dimensionless number that represents the behavior of suspended particles in a fluid [38]. The smaller the value of St_i^h, the lower the inertia of the droplets, the easier it is to follow the fluid movement and the more pronounced its diffusion. St_i^h for the head can be calculated as:

$$St_i = \frac{\frac{v_{gc}}{2}}{\frac{d_h}{2}} \frac{\rho_d {d_{di}}^2}{18\mu_g} \tag{8}$$

$$v_{gc} = 6.2 v_0 \frac{d_m}{s} \tag{9}$$

where ρ_d is the density of droplet; d_{di} is the diameter of droplet group; μ_g is the gas dynamic viscosity; d_h is the head diameter; v_{gc} is the Gaussian centerline velocity, which is related to the initial velocity of the droplets (v_0), the diameter of mouth (d_m), and the centerline length (s) of jet travel, which is close to the value of x.

2.4.2. Short-range airborne route

The accumulate exposure dose by short-range airborne route at time, $D_{SR}(t)$ can be calculated as [35,36]:

$$D_{SR}(t) = \int_0^t E_{SR}dt \tag{10}$$

$$E_{SR}(x) = \sum_{i=1}^{16} n_{xi}^{I} \bullet V_i \bullet AE_i \bullet \rho_v \bullet (1 - q_{ma}) \tag{11}$$

where $E_{SR}(x)$ is the exposure dose at distance x from the infected individual; n_{xi}^{I} is the number of droplets in the inhalation zone at distance x; AE_i is the aspiration efficiency; ρ_v is the virus density in droplets; q_{ma} is the filtration efficiency of the mask for aerosols.

$$AE_i = 1 + \left(1 - \frac{1}{1 + k_c St_i^c}\right)\left(\frac{{d_m}^2}{\left(d_h \sqrt[3]{\frac{\varphi}{3}}\right)^2} - 1\right) \tag{12}$$

$$\varphi = \frac{{d_m}^2 v_{in}}{{d_h}^2 v_{gc}} \tag{13}$$

where St_i^c is the Stokes number in the convergent part at distance x; the constant k_c takes the value 0.3; v_{in} is the velocity of the inhaled droplets; φ is the sampling ratio, which depends on the diameter of the head (d_h) and mouth (d_m), the jet velocity (v_{gc}) at distance x and the inhalation velocity (v_{in}) of the individual.

2.4.3. Long-range airborne route

Aerosol particles <10 μm can be suspended in the air and move with the airflow [39], especially those <5 μm can be directly inhaled into the alveoli [40]. Small droplets are rapidly reduced to about 1/3 of their volume by evaporation after being emitted [41]. Therefore, droplets with an initial diameter of less than 30 μm were considered in the long-range airborne route. The calculation of long-range airborne exposure dose at time, $D_{LR}(t)$ is as follows [35]:

$$D_{LR}(t) = \int_0^t E_{LR} dt \tag{14}$$

$$E_{LR}(t) = \sum_{i=1}^{6} v_{in} \bullet C_i(t) \bullet \rho_v \bullet (1 - q_{ma}) = \sum_{i=1}^{6} v_{in} \bullet \frac{n \bullet n_{0i} V_i}{q_r V_r} (1 - e^{-q_r t}) \bullet \rho_v \bullet (1 - q_{ma}) \tag{15}$$

where $E_{LR}(t)$ is the long-range airborne exposure dose at time t; C_i is the airborne fine droplet concentration in the inhalation zone; n is the number of infected; n_{0i} is the number of droplet with diameter i emitted by one infected individual; q_{ma} is the filtration efficiency of masks; $q_r = q_v + q_f + q_d + q_a + q_{in}$ is the droplet removal rate due to ventilation (q_v), filtration (q_f), deposition (q_d), virus decay in aerosols (q_a), and inhalation by susceptible individuals (q_{in}); V_i is the volume of single droplet; V_r is the volume of the zone.

The q_v depends on the zone ventilation rate, which is usually expressed by the number of Air Changes per Hour (ACH). ACH is the most critical parameter affecting the indoor airborne spread of viruses [15]. In this study, it is assumed that the building is mechanically ventilated with mixing ventilation (MV) combined with air filtration units. Previous studies have shown that the air temperature and particle number concentrations under MV systems are homogeneous with low indoor air velocities [42]. Considering that multi-zone buildings consist of multiple interconnected rooms, CFD simulations are difficult to set boundary conditions and consume a lot of computational resources, related studies usually assume a uniform distribution of aerosol particles in each zone [18, 19]. Therefore, this paper assumes that the droplet concentration in the region is uniformly distributed, but combined with the actual situation, the particle concentration in the individual inhalation region C_i is reasonably corrected [35]:

$$C_i = \left(\frac{1}{32.5\%}\right)^3 C_z \tag{16a}$$

where C_z is the zonal droplet concentration.

2.4.4. Fomite route

The accumulate exposure dose by fomite route at time, $D_F(t)$, can be calculated by Ref. [10]:

$$D_F(t) = \int_0^t E_F dt \tag{16b}$$

$$E_F(t) = D_h(t) \bullet TE_{hf} \bullet \gamma_{hf} \bullet A_{hs} \bullet A_{hf} \bullet \rho_v \tag{17}$$

$$D_h(t) = D_h(t - \Delta t) + D_s(t - \Delta t) \bullet TE_{sh} \bullet \gamma_{sh} \tag{18}$$

$$D_s(t) = D_s(t - \Delta t)(1 - q_s) + D_h(t - \Delta t) \bullet TE_{sh} \bullet \gamma_{sh} \bullet A_{hs} \tag{19a}$$

where $D_h(t)$ is the viruses on hands, as shown in Eq. (17). Note that $D_h(t)$ is 0 if the susceptible individual washes his hands at time t. TE_{hf} is the transfer efficiency between hands and facial membranes; γ_{hf} is the probability of touching facial membranes; A_{hs} is the contact area between the hand and the surface; A_{hf} is the area during the hand-to-membrane contact; $D_s(t)$ represents the viruses on contaminated surfaces and is calculated by Eq. (18); TE_{sh} is the transfer efficiency between surfaces and hands; γ_{sh} is the probability of touching surface; q_s is the virus decay rate on surfaces.

2.5. Risk calculation

Dose-response model is used for the assessment of infection risk from the multi-route transmission, including droplet, airborne and fomite transmission [10]. The total infection risk through multi-route transmission can be calculated as:

$$P = 1 - \exp\left(-\frac{(D_{LD} + D_{SR} + D_F + D_{LR})}{k}\right) \tag{19b}$$

where P (%) represents the infection probability of the susceptible individual, D_{LD}, D_{SR}, D_F, D_{LR} are cumulative exposure doses due to large droplet route, short-range airborne route, long-range airborne route, and fomite route, respectively; k is the infectious dose. In addition, the Zone Cumulative Virus Exposure (ZCVE) was used to characterize the risk level of the zone. The ZCVE of Zone i at time, $ZCVE_{it}$, can be calculated as:

Table 3
Parameters in the model.

Parameters	Description	Value (s)/Distribution	Ref.
Space-related parameters			
T	Air temperature	25 °C	
T_s	Surface temperature	20 °C	
RH	Relative humidity	45 %	
ρ_a	Air density	1.189 kg/m^3	[41]
Occupant-related parameters			
A_e	Area of eyes	6 cm^2	[35, 43]
A_n	Area of nose	2 cm^2	[35, 43]
A_m	Area of mouth	π cm^2	[35, 36]
A_h	Area of head	1300 cm^2	[35, 44]
A_f	Area of finger	1 cm^2	[45]
d_0^{cough}	Droplets' initial diameters (coughing once)	[1.5; 3; 6; 12; 20; 28; 36; 45; 62.5; 87.5; 112.5; 137.5; 175; 225; 375; 750; 1500] μm	[33, 46]
d_0^{talk}	Droplets' initial diameters (counting once from '1' to '100')	[1.5; 3; 6; 12; 20; 28; 36; 45; 62.5; 87.5; 112.5; 137.5; 175; 225; 375; 750] μm	[33, 46]
d_h	Diameter of head	20 cm^2	[35, 44]
d_m	Diameter of mouth	2 cm^2	[35, 36]
n_0^{cough}	Droplets' initial numbers (coughing once)	[50; 290; 970; 1600; 870; 420; 240; 110; 140; 85; 48; 38; 35; 29; 34; 12; 2]	[33, 46]
n_0^{talk}	Droplets' initial numbers (counting once from '1' to '100')	[1; 13; 52; 78; 40; 24; 12; 6; 7; 5; 4; 3; 2; 1; 3; 1]	[33, 46]
q_{in}	Inhalation rate	0.023 m^3/min	[47]
v_0^{cough}	Initial velocity of droplets exhaled from coughing	11.7 m/s	[33]
v_0^{talk}	Initial velocity of droplets exhaled from talking	3.9 m/s	[33]
v_{in}	Inhalation velocity	1.1 m/s	[35]
v_{waik}	Pedestrian moving speed	1.4 m/s	[48]
Virus-related parameters			
k	Infectious dose	4.1×10^2	[49]
k_c	Constant	0.3	[35]
q_{ma}	Filtration efficiency of the mask for aerosols	95 %	[50, 51]
q_{md}	Efficiency of mask filtration for large droplets	46 %	[35]
TE_{hf}	transfer efficiency between hands and facial membranes	0.35	[45]
TE_{hs}	transfer efficiency between hands and surfaces	3×10^{-3}	[52, 53]
q_a	Viruses' decay rate in the air	1.27×10^{-4}/s	[11, 54]
q_p	Viruses' decay rate on the plastic	2.04×10^{-5}/s	[11, 55]
q_s	Viruses' decay rate on the steel	2.47×10^{-5}/s	[11, 55]
ρ_v	Virus density in droplets	2.35×10^9 RNA copies/mL	[56]
γ_{hf}	Frequency of hand touching facial membranes	0.4/min	[57]

$$ZCVE_{it} = \sum_{t=1}^{k} \sum_{j=1}^{n} D_{jt}^{i} \tag{20}$$

where D_{jt}^{i} is the cumulative exposure dose via four routes of occupant j at time t in Zone i.

2.6. Boundary conditions

For the rigor and simplicity of the model, this paper sets the boundary conditions for the space, people and viruses involved in the model as follows:

(1) Building space. It is assumed that there is no residual risk of propagation in the space before the simulation starts. The floor plan used in the model can only be composed of straight lines, and curved planes can be appropriately divided into straight lines, such as using octagons instead of circles. The building is assumed to be mechanically ventilated, and natural ventilation is not considered for the time being, and its ventilation mode is mixing ventilation combined with air filtration devices. The calculation process was independent for each zone, and air exchange between zones and vertical temperature stratification were not considered yet. Aerosols are uniformly distributed beyond a 2-m radius from the infected person was assumed, but a correction was made for concentrations within the susceptible individuals' inhalation zone.

(2) Occupant behavior. Since the behavioral scheduling of the Markov chain used in this study has no memory characteristics, activity chains consisting of two activities were not considered. It is assumed that each occupant is familiar with the building and can quickly find the shortest path to any destination. The occupants are assumed to be of the same height, all droplets are sprayed at an average human height of 1.7 m, and susceptible individuals are assumed to keep their eyes, nose, and mouth open when they are in close contact to an infected person. Individual differences in susceptibility (e.g., age and vaccination status) are not considered. Individuals sitting next to each other are assumed more likely to talk face to face. It is assumed that individuals who may be infected during the simulation of a workday are temporarily noninfectious and secondary transmission does not occur.

(3) Virus transmission. It is assumed that the four routes of transmission are independent of each other and that viruses entering the body by different routes were considered to have equal dose-response indices. All sizes of droplets were assumed to be spherical so that the volume could be calculated from the diameter, and that the virus concentration in droplets of different sizes was the same. Resuspension and other subsidence of droplets were ignored, and the outdoor concentration of droplet nuclei was assumed to be zero. The inactivation of virus during droplet evaporation is not considered, i.e., the viral load of a person exposed to a droplet is the same as the viral load at the instant the droplet is exhaled.

The parameter settings involved in the model are demonstrated in terms of space-related, occupant-related and virus-related parameters, as shown in Table 3.

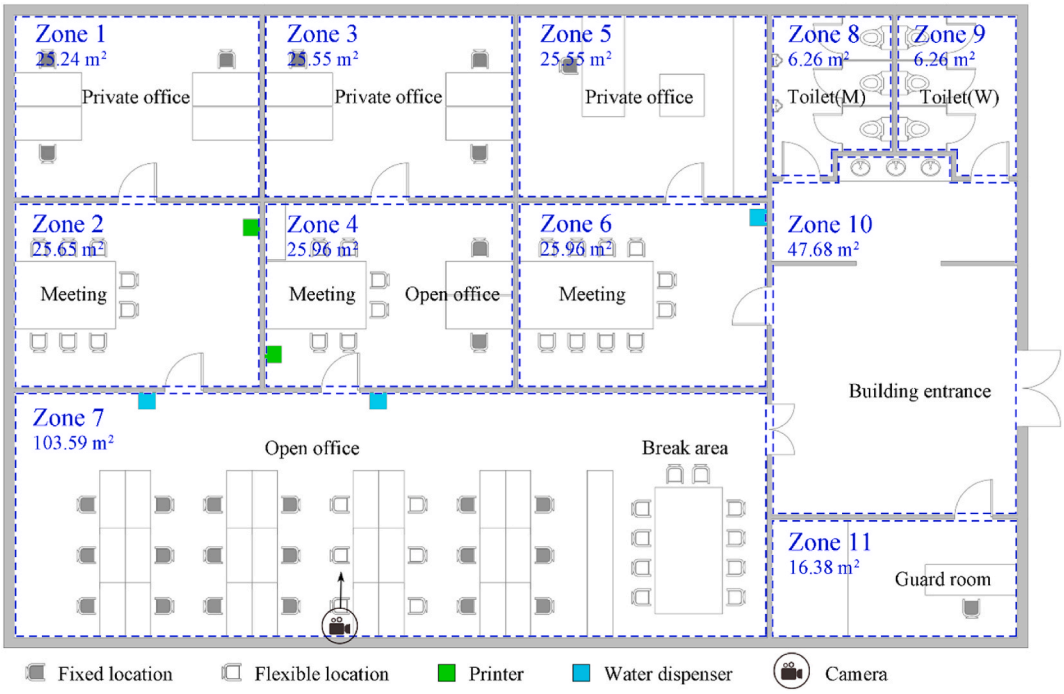

Fig. 5. The floor plan of the office.

3. Case study

3.1. Building information

A university office building in Tianjin, China was selected as a case study. The building contained two parts: laboratory and office. The floor area of the office was about 342 m^2, which contained a small mezzanine floor that was not considered in this study. The floor plan of the office space is shown in Fig. 5. It was divided into 11 zones, and the floor area of each zone was measured, and the room height was 3 m. The office building was predominantly displacement ventilated (inlet and outlet on the opposite side) with occasional natural ventilation. The ACH was set to 5. The grey and white seats in Fig. 5 represented fixed and flexible positions, respectively. There were three water dispensers and two printers, which were in the open-plan office area and the conference room.

Environmental surfaces observed to be touched by multiple occupants in the office building included doorknobs, water dispenser buttons, and printer buttons. Although toilet flush buttons and stall door handles were also frequently touched, individuals generally washed their hands immediately after exiting the toilet stall. Almost no one touched their face during this brief period, and the virus will be cleared after washing hands. Therefore, the environmental fomite sub-route in the model involves touching door handles, printers, water dispensers, and hand washing.

3.2. Behavior data collection and model validation

The daily occupancy of the office was 30, consisting of 6 teachers, 23 students, and 1 janitor. The occupant behavior data used in the model mainly came from observations and questionnaires. The surveys included information on basic schedules, meeting arrangements, and time-independent activities.

Occupants of this university office are categorized into three role groups: teachers, students, and janitors. Their basic schedule consists of the time of arrival, departure, and lunch (see Table 4). There were three teams, and they met on average once a week, each lasting about an hour (see Table 5). Individual time-independent activities mainly involved going to the water dispenser, printing, going to the toilet and taking a break. Their durations and intervals are shown in Table 6. The rest of the time was spent working at one's location. After inputting these behavioral data into the model, the activity schedule for all occupants during a working day was simulated.

The model was validated by comparing simulation results with actual observations. The validation of the model included basic schedule, room occupancy, pedestrian walking speed and trajectory (Fig. 6). Occupant behavior data was recorded by a camera in Zone 7 for 3 days, and its location was shown in Fig. 5.

Fig. 6 (a) shows the time distribution and average values from simulated and observed basic occupant schedules respectively. The distribution of arrival and lunch times is roughly similar, with an average difference of no more than 2 min. The actual departure time of occupants was concentrated after 18:00, which was an average of 14 min later than the simulated time. The simulated average time that occupants spent indoors was 8 h and 20 min. Compared with the measured 8 h and 30 min, the error is about 2.0 %, which is acceptable.

For the room occupancy, the simulated and measured occupancy status of Zone 7 on a working day is shown in Fig. 6 (b). The main difference is that the actual meeting time is earlier. In addition, due to the absence of some people, the actual total number of people present was less than the simulation. The Pearson correlation coefficient was used to calculate the correlation between the 2-time series, and its value was 0.91 ($P = 3.35e\text{-}249$). It shows a significant correlation, which means that the simulation results are relatively close to the actual measurements.

For pedestrian walking speed, it can be calculated by spatial coordinate transformation [58]. The pedestrian walking distance in millimeters is extracted from the video for each time step and converted to real-world distance in meters. 10 video clips (5s × 10 frames/s) were selected. The occupant coordinates in the video coordinate system were manually marked with the mouse and converted into world coordinate P_i. Data was collected every 0.2 s (2 frames) as shown in Fig. 6 (c). The speed v_i can be calculated by the following equation:

$$v_i = \frac{||P_{i+1} - P_i||}{[0.2 * (T_{i+1} - T_i)]} \tag{21}$$

where $||P_{i+1} - P_i||$ represents the distance between points P_{i+1} and P_i, T_{i+1} and T_i were the time series. The average measured data was 1.32 m/s, which was agreement with the 1.4 m/s used in the model.

For the pedestrian trajectory, the trajectories of pedestrians in Zone 7 were plotted based on video clips from 8:00 to 9:00 a.m. It can be seen from Fig. 6 (d) that the actual trajectory was relatively consistent with the simulated walking navigation line. Possible deviations are caused by each person's walking habits, while the motion characteristics of the occupants in the model are defined to be similar.

Table 4
Basic schedule.

Roles	Arrival		Departure		Lunch		
	Start	Variation (min)	Start	Variation (min)	Start	Variation (min)	Duration (min)
Teacher	08:30	15	17:30	15	12:30	10	60
Student	08:30	15	18:00	15	12:00	10	60
Janitor	07:30	15	18:30	15	13:00	10	60

Table 5
Team information and meeting schedule.

Team	Teacher	Student	Zone	Duration (min)	Frequency
1	4	6	Zone 6	60 (±5)	1/week
2	1	5	Zone 4	60 (±5)	1/week
3	1	7	Zone 2	60 (±5)	1/week

Table 6
Time-independent activity information.

Roles	Duration/interval (min)				
	Working	Going to toilet	Getting water	Printing	Having a break
Teacher	30/-	3/120	2/120	2/240	10/240
Student	30/-	3/120	2/120	2/240	10/240
Janitor	60/-	3/120	2/120	2/480	–

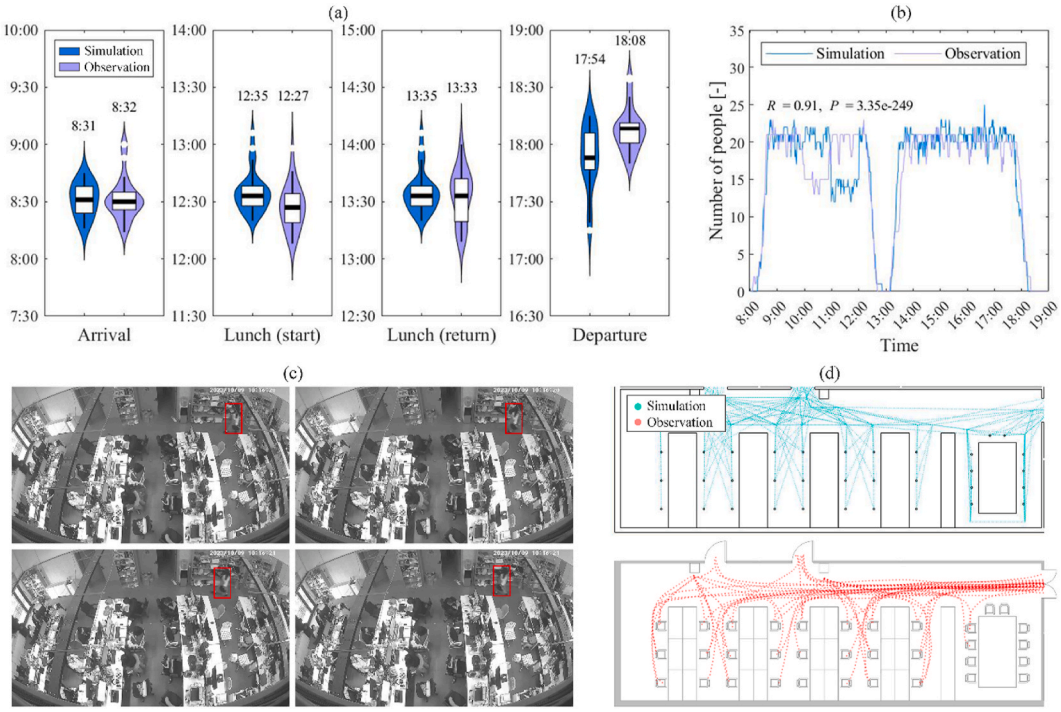

Fig. 6. Validation of the model. (a) Simulated and observed basic schedules of occupants. (b) Simulated and measured occupancy status of Zone 7 on a working day. (c) The occupant coordinates in the video coordinate system were manually marked with the mouse every 0.2 s. (d) The actual trajectory and the simulated walking navigation line.

The observed movements of the occupants were recorded and compared with the navigational paths generated by the model. As shown in Fig. 6 (d), the trajectories of occupants' movements obtained from the simulation are similar to those recorded from the field study. Possible deviations are caused by each person's walking posture and head swing. Note that the motion characteristics of occupants are similar in the model.

3.3. Non-pharmaceutical interventions and scenario settings

The effects of non-pharmacological interventions in reducing the infection risk of this university office building were assessed at different operational levels, including spatial layout, ventilation, and behavioral control (Fig. 7). The spatial layout included three aspects: zone layout, furniture layout and facility layout. Compared with the baseline scenario, three types of zone layouts are set up according to the degree of openness of the space. The arrangement of the desks in the open-plan office space was changed in the furniture layout. Three common office desk layouts were selected, including one-way linear bench desk, L-shaped desk, and Y-shaped desk. Water dispensers and printers in both facility layouts were located entirely in open-plan office area or meeting rooms, respectively. Ventilation interventions included changes in air exchange rate (ACH) and filtration efficiency (FE). Behavioral controls

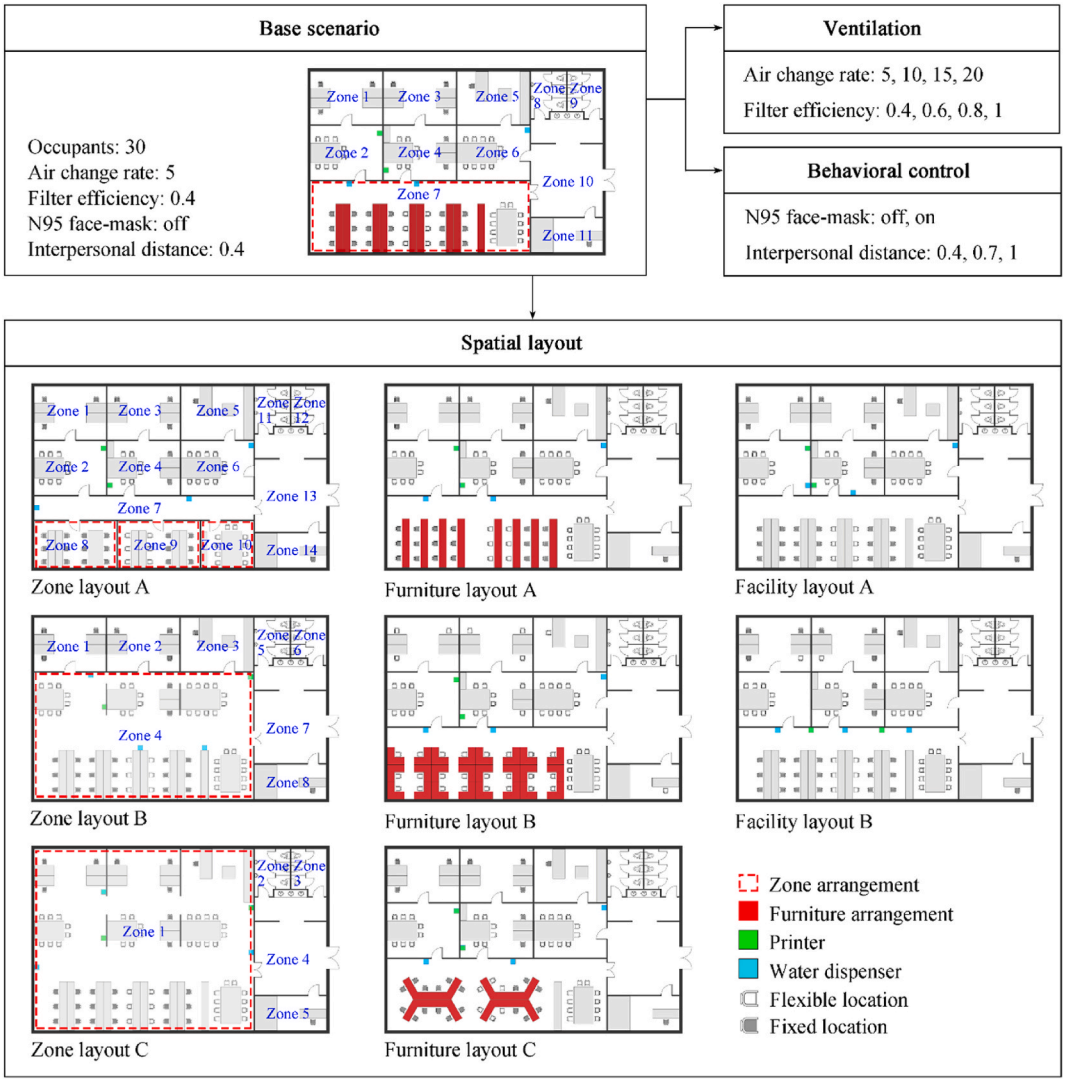

Fig. 7. Scenarios with different ventilation, behavioral controls, and spatial layouts.

included wearing N95 masks (WM) and maintaining interpersonal distance (ID), which represent individual and group behaviors, respectively. In addition, a scenario was set up where surface cleaning (SC) is performed every 4 h. A total of 20 scenarios were set up, with the settings and coding shown in Table 7. Each scenario was simulated 30 times to reduce the fluctuation of results due to randomness, for a total of 600 simulations.

The optimal combination of each type of intervention was selected for further simulation to investigate and compare the effects of the combined measures. The scenarios were set up as shown in Table 8, with C1 and C2 representing combinations of behavioral interventions in the base scenario, and combinations of ventilation interventions, respectively. C3 refers to spatial layout combinations, i.e., combinations of optimal design of space, furniture, and facility layouts.C4 represents the combined scenario of optimal spatial layout, optimal ventilation and filtration solutions, and optimal behavioral control measures. Each scenario was simulated 30 times for a total of 120 simulations.

4. Results

4.1. Spatial risk analysis of base scenarios

4.1.1. Occupants' contagion-related behaviors

The distance between individuals was calculated based on their spatio-temporal trajectories, and then the distribution of locations and times of close contact can be obtained. Fig. 5 shows the simulation results for a student as a randomly infected individual. After one working day of exposure, most of the potentially exposed individuals were distributed in the same zone as the infected. Some of them were located close to the infected, and others had overlapping activity schedules, such as attending the same meeting. Close contact

Table 7
Scenario settings and coding.

Layout	ACH	FE	WM	ID	SC	Code
	5 10 15 20	0.4 0.6 0.8 1.0	0 50 % 100 %	0.4 0.7 1.0	no per 4 h	
Base layout	*	*	*	*	*	B
Room layout A	*	*	*	*	*	Z2
Room layout B	*	*	*	*	*	Z3
Room layout C	*	*	*	*	*	Z4
Furniture layout A	*	*	*	*	*	Fu2
Furniture layout B	*	*	*	*	*	Fu3
Furniture layout C	*	*	*	*	*	Fu4
Facility layout A	*	*	*	*	*	Fa2
Facility layout B	*	*	*	*	*	Fa3
Base layout	*	*	*	*	*	A2
Base layout	*	*	*	*	*	A3
Base layout	*	*	*	*	*	A4
Base layout	*	*	*	*	*	E2
Base layout	*	*	*	*	*	E3
Base layout	*	*	*	*	*	E4
Base layout	*	*	*	*	*	M2
Base layout			*		*	M3
Base layout	*	*	*	*	*	I2
Base layout	*	*	*	*	*	I3
Base layout	*	*	*	*	*	S2

Table 8
Combined scenario settings and coding.

Layout	ACH	FE	WM	ID	SC	Code
	5 10 15 20	0.4 0.6 0.8 1.0	0 50 % 100 %	0.4 0.7 1.0	no per 4 h	
Combined layout	*	*	*	*	*	C1
Base layout	*	*	*	*	*	C2
Base layout	*	*	*	*	*	C3
Combined layout	*	*	*	*	*	C4

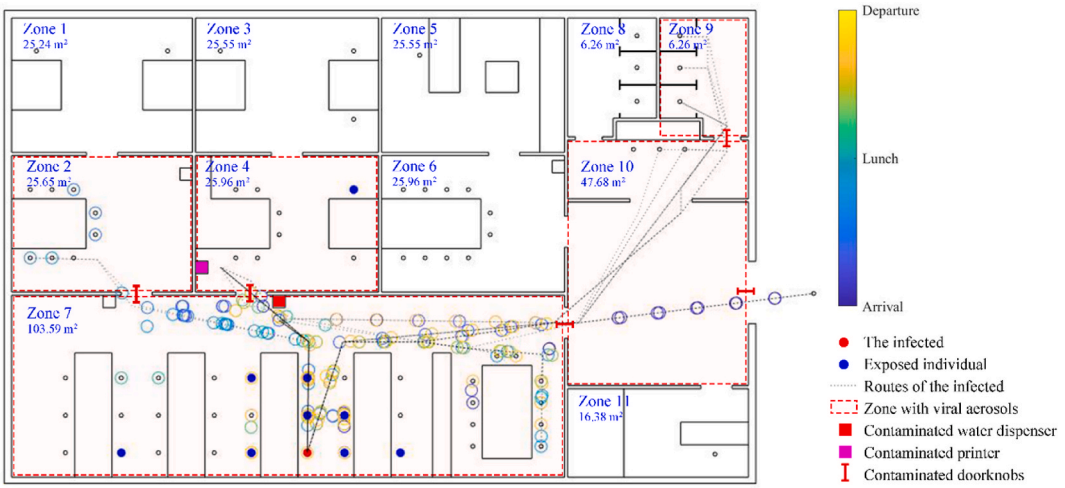

Fig. 8. Close contact, environmental contamination, and distribution of exposed individuals in the baseline scenario. Colored circles represent locations where close contact occurred throughout the day, and their color represents the time occurred. Environmental contamination refers to zones with viral aerosols and contaminated environmental surfaces, including water dispensers, printers, and doorknobs. (For interpretation of the references to color in this figure legend, the reader is referred to the Web version of this article.)

occurred primarily in zone 7, where he or she spent the most time. In Zone 7, close contact was mainly observed around locations where activities such as working, resting, getting water take place, as well as on the way to these locations, and its temporal distribution is not centralized. Zone 2 is a conference room where short-range exposures were related to the meeting schedule and its location was close to the seats. Close contact at the building entrance (Zone 10) mainly occurred during arrival, departure and

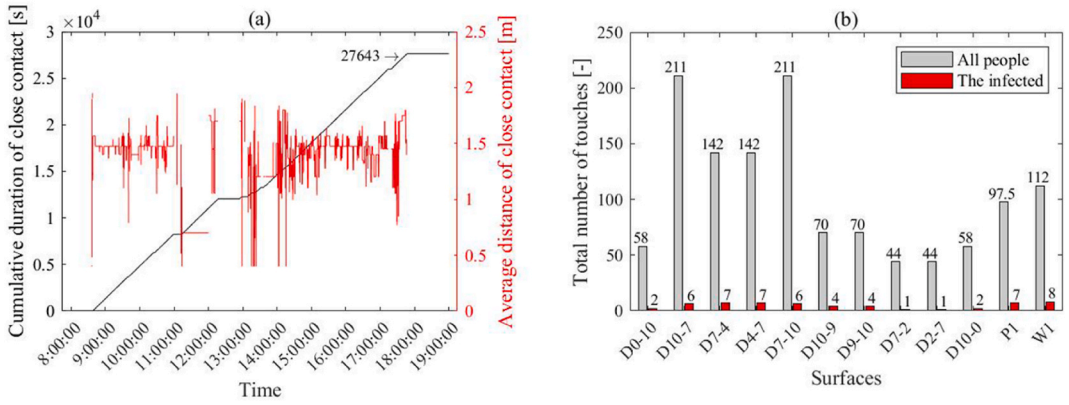

Fig. 9. (a) Cumulative duration and real-time average distance of close contact between the infected with others. (b) The number of times all contaminated surfaces were touched.

lunchtime, and its location was distributed on the line connecting the entrance to Zone 7. As shown in Fig. 9 (a), the cumulative duration (about 1070 min) and real-time average distance of close contact were calculated. Since the boundary distance of 2 m for close contact was larger than the distance between two adjacent seats in the open-plan office workspace, two occupants may be in constant close contact while working, and the accumulated time obtained is relatively long. The average distance of close contact between occupants throughout the day fluctuated mainly around 1.5 m, with a minimum of 0.5 m. During the meeting from 11:00 a.m. to 12:00 a.m., the value was only 0.8 m because the seats in the meeting room were closer.

Fig. 9 (b) shows the number of times all contaminated surfaces were touched by susceptible and infected individuals respectively. Their distribution and frequency of being touched were related to activities such as arrival, departure, going to the toilet, printing, etc., depending on the individual and group schedules. The most frequently touched doorknobs were between zones 7 and 10, which were touched 211 times, followed by doorknobs between zones 7 and 4, which were touched 142 times. Note that Zone 4 was frequently visited because it contains a printer, which is closer to the open-plan office workspace than the other printer in Zone 2. The same goes for the water dispenser in Zone 7.

4.1.2. Virus spread and exposure risk

The locations of the infected individual's activities involved five rooms. Fig. 10(a) shows the airborne virus concentration variations in the five zones involved in the trajectory of the infected. These curves showed obvious spatial and temporal heterogeneity, which was closely related to occupants' activity schedules and the ACH of the room. The infected individual spent a lot of time working in Zone 7, and the virus emission rate was greater than the dilution rate, therefore its concentration gradually rose throughout the day to eventually reach approximately 1×10^{-5} μL/m^3. The virus concentration in Zone 2 increased rapidly to about 5×10^{-5} μL/m^3 between 11:00 a.m. and 12:00 a.m., when the infected individual's group had a meeting, far exceeding that in Zone 7. High frequency talking during the meeting led to an increased virus emission rate, and the small size of Zone 2 resulted in a rapid rise in viral concentration. The virus concentrations in Zone 9 and Zone 4 repeatedly increased and then decreased over several periods. This is because the infected individual entered these two rooms many times, stayed for a few minutes and then left, and the virus in the air was diluted in almost an hour. Zone 10 was the building entrance, where occupants were just passing by and not staying, so the risk of long-range airborne exposure was minimal.

The cumulative pollution level of environmental surfaces is shown in Fig. 10(b), with doorknobs being the highest, up to more than

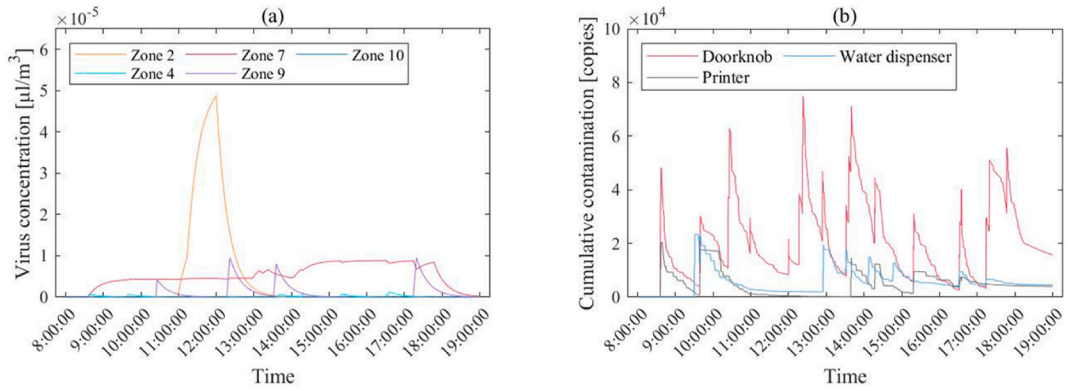

Fig. 10. (a) Virus concentration in different zones; (b) Cumulative contamination levels of three environmental surfaces.

7.0e+4 copies, followed by water dispenser buttons and printer buttons, up to more than 2.0e+10 copies. Combined with Fig. 9(b), changes in surface viruses were related to the time and number of contacts. The changing trends of the three types of surfaces were generally similar. Virus decay and frequent contact with other occupants resulted in a rapid reduction of the virus on the surface until the next touch by the infected.

Fig. 11 (a) shows the real-time zone cumulative virus exposure, ZCVE, of five zones visited by the infected, i.e., the cumulative virus dose intake by all susceptible individuals in the area through four transmission routes. After one working day, Zone 7 had the highest ZCVE of 1.5e+7, followed by Zone 2 and Zone 10, with 8.9e+5 and 1.1e+5, respectively. The ZCVE of Zone 7 and Zone 10 increased rapidly when occupants arrived at the building, and then the value of Zone 7 continued to increase, while that of Zone 10 remained. The value of zone 2 increased from 11:00 until 12:00 and exceeds that of zone 10 at approximately 11:20. Comparing the distribution of close contacts in Fig. 5 and the virus in Fig. 7, it can be found that ZCVE mainly depends on the number and duration of close contact, followed by aerosol concentration. Zone 9 was a toilet with the lowest overall exposure dose because the partition effectively blocks short-range exposure. The cumulative exposure of the three role groups was compared in Fig. 11 (b). The student group had the highest values of 1.1e+6 because they were the most numerous and mostly worked in the same zone, with a higher probability of close contact. Additionally, when the infected individual was a teacher, the ranking of the contributions of the four transmission routes remained, while the overall exposure dose decreased.

Short-range airborne transmission dominated the four exposure routes with 87.9 %, followed by large droplet deposition with 12.0 % (Fig. 12 (a)). The exposure dose from the long-range airborne route was less than one-thousandth of that from the short-range airborne route. The contamination level of environmental surfaces was relatively high, yet the dose of virus intake by occupants through the fomite route was very low. Droplets released by coughing and talking were considered in the short-range exposure. This study assumed that the infected individual coughs every five minutes, and the frequency of talking depends on the activity type and distance from others., the distance decreased, the likelihood of conversation between occupants increased, and the frequency of talking was set higher during meetings. Coughing resulted in a higher exposure dose proportion than speaking for both short-range air inhalation and large droplet deposition (Fig. 12 (b)). This is because a single cough emitted more virus particles than one second of talking.

4.2. *Effect of layout, ventilation, and behavioral interventions*

Fig. 13 shows the cumulative exposure dose, infection rate, and the fraction of the four transmission routes after 30 simulations of the 18 scenarios introduced in Section 3.3. Almost all scenarios were dominated by short-range airborne transmission (77.0%–99.9 %), followed by large droplet route (0–19.7 %), except for M2, where large droplet transmission accounted for 51.8 %.

For different spatial layout designs, changing zone layout (Z2-Z4) had the most significant impact on exposure risk among the nine scenarios related to spatial layout. Compared with the baseline scenario, the open-plan office area in Z2 was divided into three units, which effectively reduced the close contact of occupants between units, thereby reducing the infection risk from 24.6 % to 15 %. However, the reduction in room size resulted in a higher concentration of airborne viral particles in the unit where the infected was located, thus increasing long-range airborne exposure. In the Z3 and Z4 scenarios, meeting rooms and private offices were no longer separate zones, the average infection risk increased by 11.2 % and 6.8 %, respectively. Both the number of occupants in the main zone and the probability of their movement routes crossing increased. The proportion of large droplet exposure increased significantly in these two scenarios, which means that the more complex the functions of an area and the more occupants inside, the smaller the average interpersonal distance that may result in close contact. Changing the layout of furniture and equipment had a small impact on the infection risk, although they affected the movement of occupants. It was assumed that there were no baffles between desks, so short-range exposure would occur when two occupants were working in adjacent or opposite positions. In scenarios Fu2-4, the distance between occupant positions was like that in B1. Compared with B and Fa2, the exposure level in Fa3 was more than 3.5 % higher because all touchable facilities were placed in open-plan office space, increasing the possibility of crowds gathering.

In addition, the average ZCVE values for each room in the nine spatial layout scenarios were quantified, along with the number of possible exposed individuals and the distribution of the rooms in which they were located (Figs. 5–14). The results show that there is a

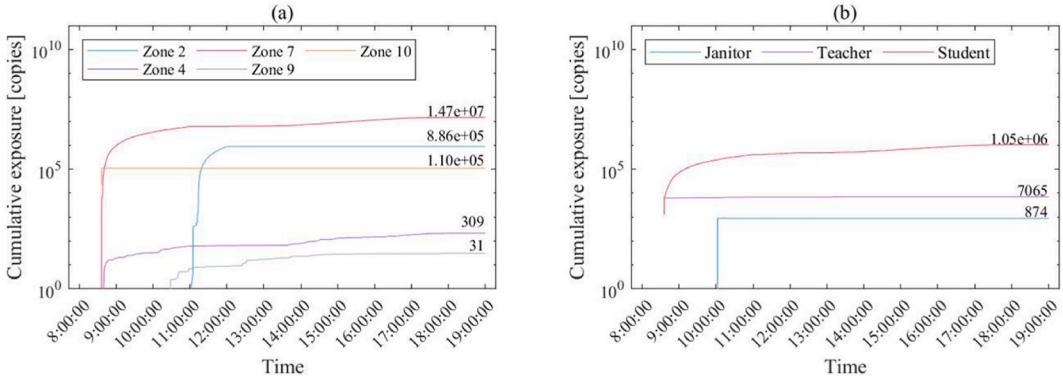

Fig. 11. (a) Cumulative exposure doses in different zones; (b) Cumulative exposure doses for different role groups.

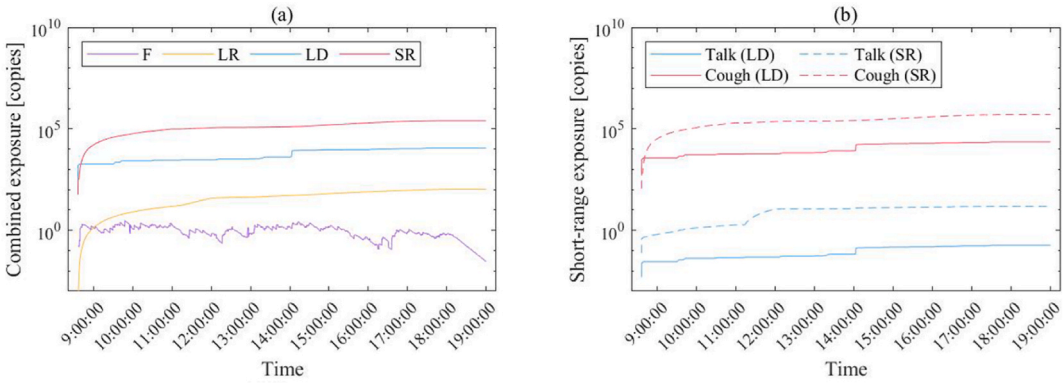

Fig. 12. (a) Cumulative exposure doses and fractions of four transmission routes; (b) Cumulative exposure doses and fractions due to talking and coughing in short-range exposure.

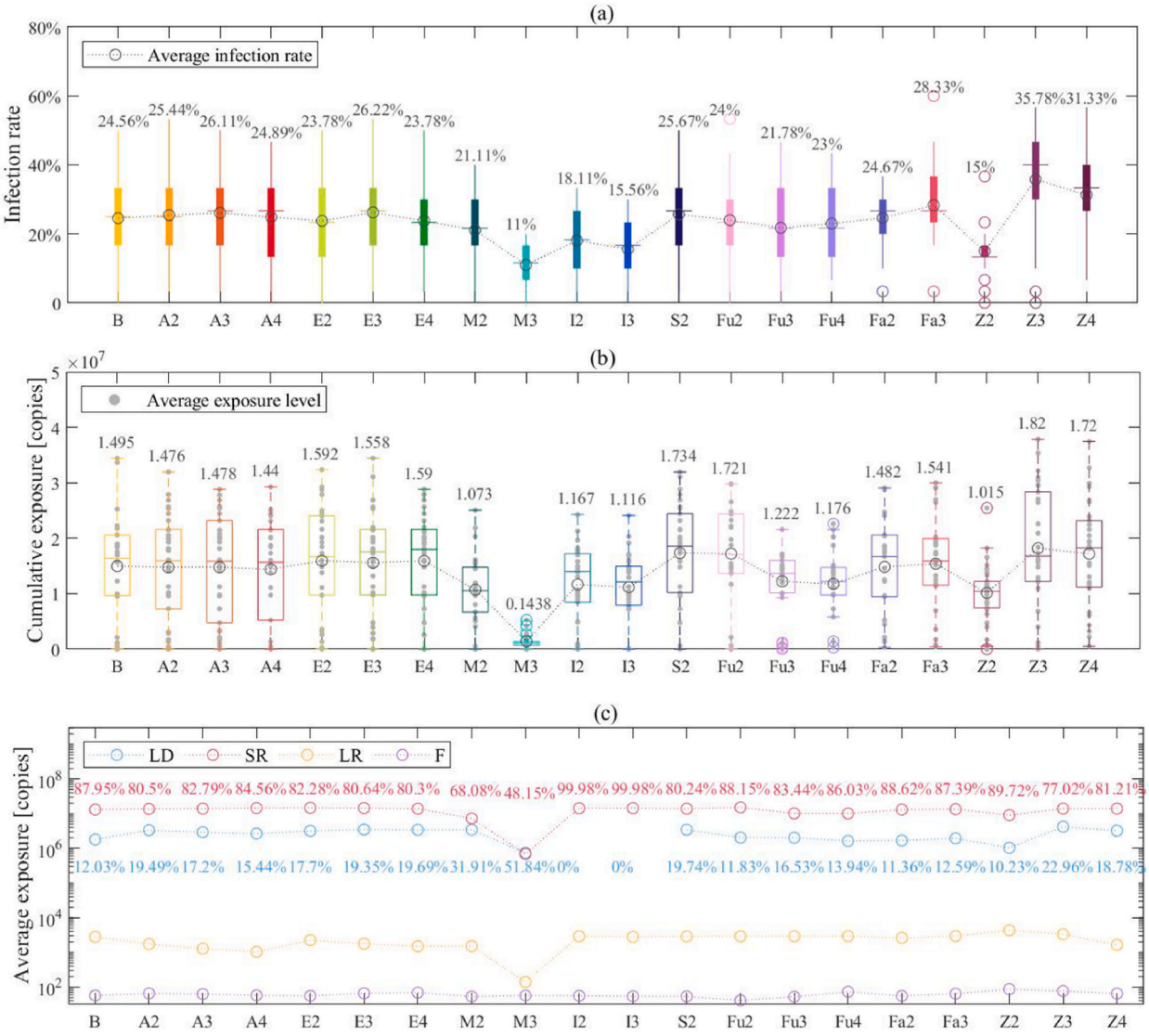

Fig. 13. (a) Infection rate, (b) exposure dose, and (c) fraction of four transmission routes within a working day for all scenarios.

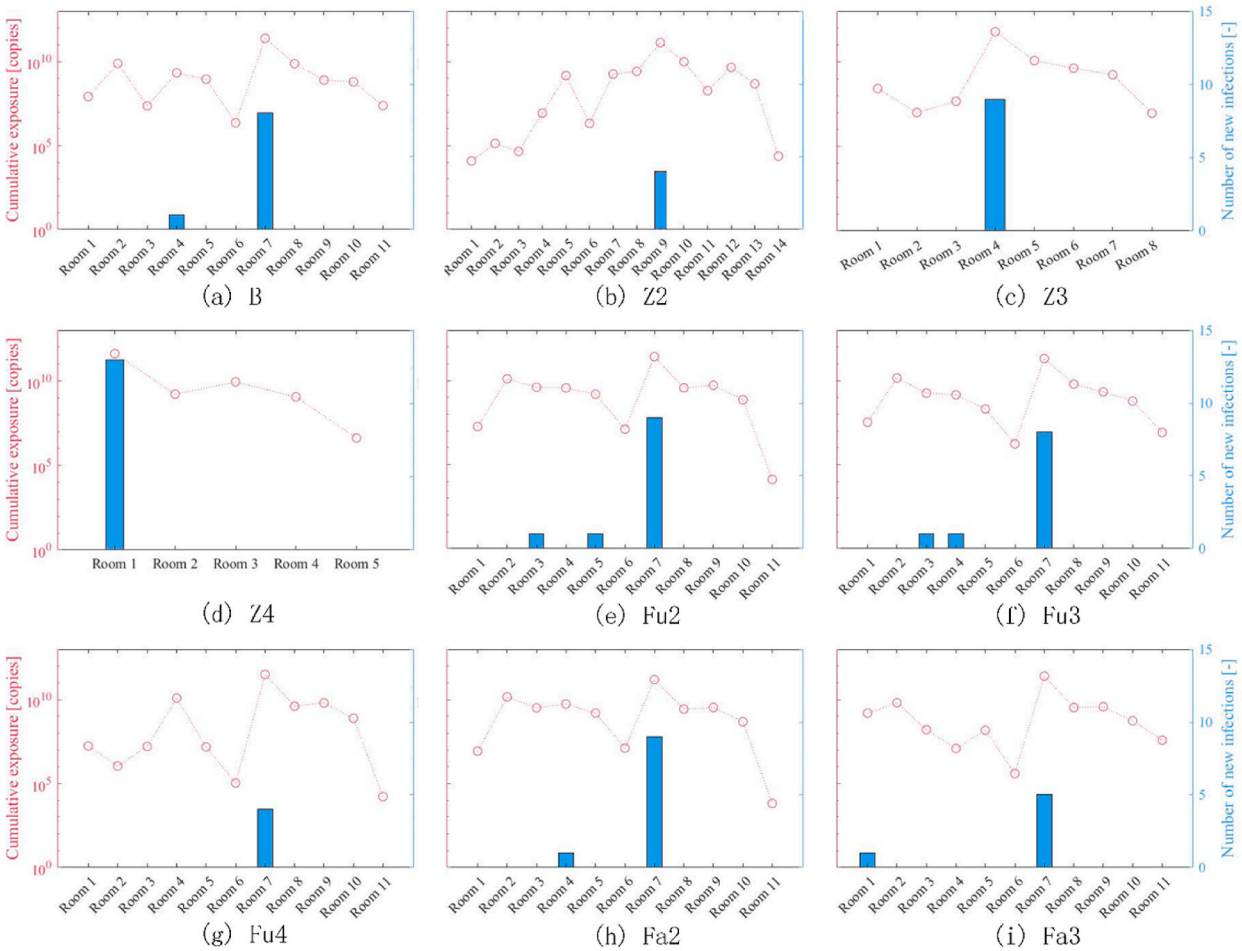

Fig. 14. Zonal level ZCVE values and distribution of exposed individuals in different spatial layouts.

strong correlation between them and that the ZCVE values of a space can be used to characterize the level of spatial risk.

By wearing masks (M2/M3) and maintaining physical distance (D2, D3), the overall exposure dose could be reduced by 0.42e+7, 1.35e+7, 0.38e+7 and 0.32e+7 copies respectively, and the possible infection rates could be reduced by 10.8 %, 6.5 % and 9.0 % respectively. The former could reduce both large droplets and short-distance airborne transmission, while the latter mainly blocked large droplets. The exposure risk in the M2 scenario was the lowest among all scenarios because the mask could reduce 95 % of the inhalation of airborne viruses and the deposition of large droplets on the oral and nasal mucosa. The reason why the mask did not completely isolate the large droplet route was that the virus was assumed to be able to enter the human body through the eye mucosa and cause infection.

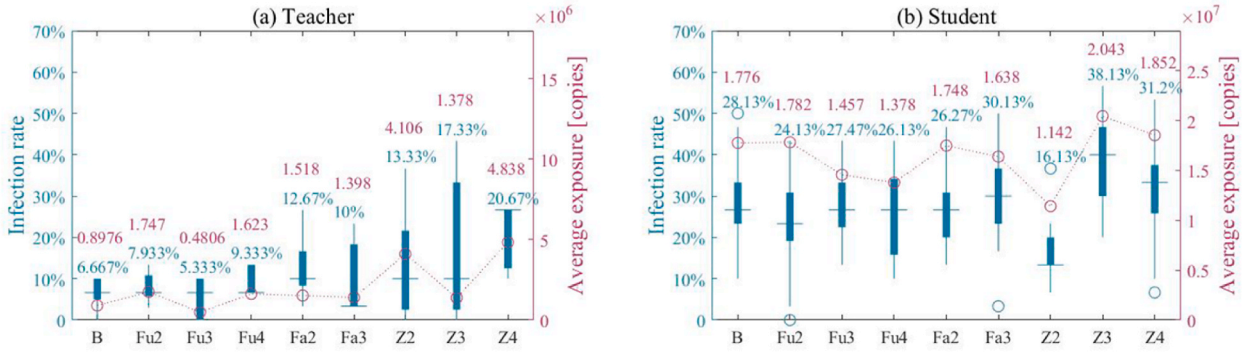

Fig. 15. Infection rate and average cumulative exposure of different role groups.

Increasing ACH and filtration efficiency helped reduce virus concentrations in rooms, thereby reducing long-range airborne exposure doses (see Fig. 13 (b)). However, it had a limited effect on reducing final exposure doses and infection rates in situations where virus short-range airborne transmission predominated.

In this study, the environmental contaminant transmission pathway accounted for a small percentage of the environmental surfaces studied, despite relatively high levels of contamination. For surfaces that are touched about 10 times per hour, most pathogens are transferred from the surface to the hands of the occupants within an hour and cleaning the surface every 4 h (S2) is not effective.

Furthermore, the impact of spatial layout on the overall exposure risk of two main role groups was analyzed (Fig. 15). Compared with students' groups, the total exposure risk of teachers' group was significantly lower (except for Z2). Combined with the scenarios in Fig. 4, the two groups were present in different areas. The teachers mainly stayed in private offices, except for Z2, and their average distance from other occupants was greater/larger. Changes in furniture and facility layout showed no significant impact on exposure levels and infection risk for the student group. However, in cases Fa2 and Fa3, the teacher group's exposure risk approximately doubled because they no longer had exclusive facilities. In scenario Z2, the student office area was divided into several rooms, which effectively reduced the exposure risk of the student group (down to 16.1 %), while the risk of the teacher group was relatively increased to 13.3 %. In scenarios Z3 and Z4, the exposure risk of each group increased with the degree of openness of the space. The teacher group was more affected, with an infection rate about 3 times that of the baseline scenario, while the value for the student group was about 1.5 times.

4.3. Effect of combined interventions

After quantitatively examining single interventions, this study attempted to combine interventions to determine the potential reduction in exposure for each type of intervention. The optimal combinations for each type of intervention were (1) combination of spatial interventions (C1): zone layout A + furniture layout B + facility layout A; (2) combination of ventilation interventions (C2): ACH 20 + filtration efficiency of 1.0; (3) combination of occupant behavioral interventions (C3): mask wearing rate of 100 % + interpersonal distance of 1.0 m; and (4) combination of the above three types of interventions (C4).

The simulation results were shown in Fig. 16. The combination of occupant behavioral control measures was the most effective, reducing the average exposure dose by 1.43×10^7 and infection risk by 16.45 %. The average infection rate of office building under combined spatial design intervention and combined ventilation intervention were decreased by 10 % and 1.23 %, respectively. The multilevel combination of spatial interventions was more effective than ventilation, and also better than the separate spatial layout measures. The combined intervention solution of space, behavior, and ventilation was able to reduce the exposure dose to 4.47×10^5 and the average risk of infection to 6 %. The results confirmed the effectiveness of non-pharmacological interventions including spatial layout, occupant behavioral control, and ventilation in controlling the office building risk during an outbreak. When the outbreak is unknown, the proper space layout can reduce the number of occupant flow crossings and close connections, thus providing a good precautionary effect.

5. Discussions

5.1. Linking the occupant behavioral model to the virus transmission model

Linking occupant behavioral models to virus transmission models in current respiratory risk assessment simulations remains a challenging problem. At the city scale, technologies such as big data [59] and artificial intelligence [60]are used for crowd control and outbreak surveillance analysis in venues. Considering different virus transmission routes, behavioral models at the building scale need to be able to portray occupant movement and exposure patterns, especially with close contact. Pedestrian dynamics-based risk assessment model focuses on the effect of pedestrian parameters on social distance, such as pedestrian density and walking speed, while the probability of infection was simplified to a function related to physical distance and duration [61]. Some studies have further attempted to characterize contagion-related behaviors during occupant movement to calculate the exposure level of different transmission routes. Lee et al. [62] proposed the OccSim system, which can generate occupancy based on building plans to compare the potential impact of design factors on infection risk. Li et al. [63] integrated contaminated surfaces into the Building Information Model (BIM) and proposed a room-level environmental fomite risk prediction model. Most of the pedestrian simulations in virus transmission risk assessment models were based on a fine-grid model [62,63], with grid sizes typically ranging from 0.5 m to 1 m [10]. The smaller the size of the grid, the more detailed it expresses the transfer of information for each time step; however, the calculation time significantly increases as well.

For office buildings, occupants spend most of their time sojourning in specific locations rather than wandering randomly, so a vector-based model can be more appropriate for such scenario. MC has a significant advantage in expressing changes in human spatio-temporal behavior [27]. Occupant activity and location within the room can be considered as state variables in an MC, whose transitions over time can be quickly predicted by the stochastic processes involved. The model has a low calculation time, with a single simulation taking about 1 h, a saving of about 83 % compared to Ref. [10]. The temporal autocorrelation of occupants' activities and locations can be characterized while ensuring inter-correlation between occupants within each zone. The proposed approach generated time-activity trajectories for each occupant based on simple behavioral data and focused on calculating large droplet exposures and short-range airborne exposures when occupants were in close contact with each other. It is possible to predict the infection risk on a room, a building or even a neighborhood for a short period, rather than being limited to a small single zone of space. In addition, some studies have predicted risk in specific spaces by investigating data on people's infection-related behaviors, surveillance video can be used to detect occupant distribution [64], close contact behavior [65], and surface touch [7], and to track pedestrian trajectories [66]. Zhang et al. [7] observed touching behaviors in a university office to calculate fomite transmission risk. Yang et al.

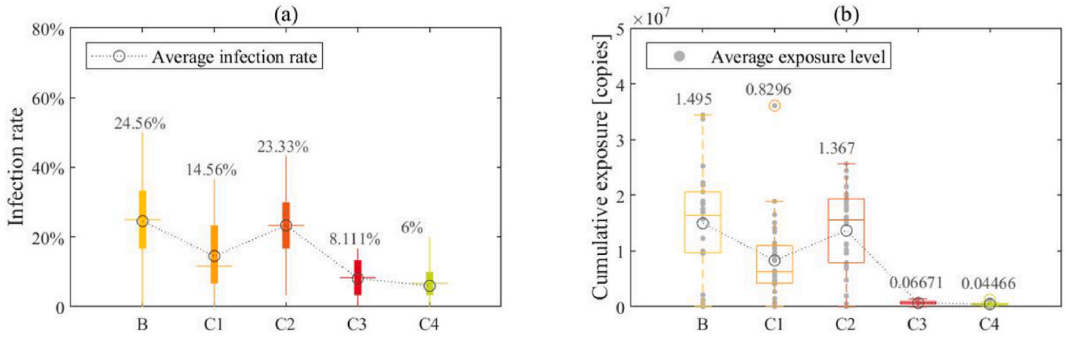

Fig. 16. Infection rate and average cumulative exposure of combined interventions.

[67] observed the close contact behavior of pedestrians to calculate large droplets and short-range airborne transmission in airports. Zhong et al. [66] captured occupant behavioral trajectories to assess on-site airborne risk in office buildings. The limitations of these methods are that they only support a particular actual building and require a large number of sensors, which is inconvenient for most public spaces, and the manual identification of videos is extremely labor intensive. However, the simulation model can be validated and optimized to improve its accuracy by analyzing and mining the data from these observations.

5.2. Spatial distribution and control of infection risk

The average cumulative infection probability on a workday could be up to 24.6 %, assuming an initial infection rate of 3.3 % (1 infected individual in a 30-person office building). Surveys have shown that one infected person in an open-plan office in Switzerland infected 67–83 % of the team [68]. Another epidemiological survey of a call center in Korea showed a 43.5 % infection rate [69]. Although offices vary in size, floor plan, working patterns and ventilation, these cases show that the infection risk in real working environments could be high.

Moreover, in the case study of this paper, short-range airborne transmission dominated the four transmission routes, accounting for more than 80 %, which follows the findings of Chen et al. [35] and Gao et al. [70]. This suggests that when calculating the indoor infection risk, it is important to focus on the exposure dose decay with distance via droplet inhalation and deposition when two individuals are in close contact, rather than using a simple judgment rule, such as the infection probability decreasing linearly with the distance between individuals.

The spatial distribution of risk mainly depends on the characteristics of contagion-related behaviors of occupants. In the university office building, occupants have frequent contact with each other because of similar activity schedules. Close contact mainly occurred between occupants in the same zone, especially in open-plan office areas. Their positions were distributed around activity-related locations and paths between them, such as seats, water dispensers, and main aisles, which was consistent with the observations of Zhong et al. [66]. Meeting rooms were also higher risk areas due to the proximity of occupants and high frequency of talking, especially during meeting times. The Zone Cumulative Virus Exposure was proposed as a spatial risk indicator that represents the cumulative exposure of all occupants in the space, which was closely related to the floor plan, occupancy, and occupant activity schedule.

Behavioral controls, i.e., mask use and maintaining interpersonal distance, can directly and significantly reduce the exposure dose, as short-range exposure is the primary route in office buildings. Wearing a mask was an individual behavioral intervention that reduced the cumulative exposure dose by 1.4×10^7. Maintaining interpersonal distance was a group behavioral intervention. Increasing the interpersonal distance from 0.4 m to 1.0 m reduced the exposure dose by 0.4×10^7. Individual behavior control is more effective and less difficult to implement than group behavioral control. Since seats in offices are usually fixed and queuing is uncommon, the spatial layout is particularly important in minimizing close contact due to its impact on occupant location and routing. For the case study in this paper, changing the zone layout (Z2) reduced the exposure dose by 0.5×10^7, which ranked second only to wearing masks. Zhang et al. [10] examined the role of spatial interventions in reducing the risk of infection in supermarkets and found that increasing exits to separate pedestrians was the most effective. Cui et al. [9] evaluated the effects of spatial factors on transmission trends and suggested that dividing the obstacle into sub-ones and distributing them evenly helped reduce infection risk. Also, furniture layout has a significant impact on airborne risk and cross-infection, and placing a table between two individuals increases the exposure risk [71]. The contribution of spatial elements to reducing the spread of epidemics varies in buildings with different patterns of occupant behavior. In general, however, the benefits of separating spaces are obvious. In contrast, inappropriate layout of furniture (Fu2) and facilities (Fa3) may increase the exposure risk.

In this study, increasing ACH significantly reduced indoor virus concentrations as well as remote airborne exposure levels. This is consistent with the findings of previous studies on ventilation to reduce airborne transmission. However, the benefit it provides in terms of mitigating the overall infection risk was limited because most previous studies on the effects of ventilation have focused on remote airborne transmission, ignoring large droplet deposition and proximal airborne transmission during close contact. Recent studies have shown that susceptible individuals may inhale small droplets when in close contact with an infected individual who is talking or coughing, and this inhalation route carries a much higher risk of infection than the remote air route [35, 70, 71]. For surfaces that are touched more than 10 times per hour, most pathogens are transferred from the surface to the occupant's hands within that hour, so frequent cleaning is required to minimize fomite exposure. Although the fomite transmission route accounted for a small

percentage in this study, cleaning environmental surfaces remains an important intervention strategy for other pathogens (e.g., *Staphylococcus aureus*) that are highly transmissible by surface contact.

5.3. Limitations

The approach has demonstrated an initial capability to simulate the spread of viruses during occupant movement in real scenarios, but there are still some limitations. First, the occupant behavior in the proposed model only includes typical activities on a typical weekday and does not consider low-probability unplanned interactions, such as receiving visitors. More behavioral data needs to be collected to optimize the model for more complex activities. Second, this study considered the variation in the size and number of respiratory droplets reaching the face of a susceptible individual from being released within the close contact range (2 m). It was assumed that infectious aerosols were uniformly distributed in a zone and that the doors between rooms were closed, ignoring airflow exchanges between zones. Moreover, only the effects of ventilation rate and filtration efficiency are considered, the diverse ventilation scenarios, including wind direction, opening schedules, natural ventilation et al. are not reflected in this model due to the limitations of the current simulation environment and significant computational resources. To better quantify the risk of indoor respiratory virus transmission, it is necessary to further characterize the spatial heterogeneity of the distribution of indoor infectious aerosols during individual movement. Airflow organization can be affected by ventilation patterns, which needs to be considered in future studies. Third, some of the medical parameters used in the model need to be supported by more experimental data, such as the viral load of droplets of different sizes, and the viral transfer rate between the hand and environmental surfaces. Finally, the modeling and comparison of the effects of the three types of interventions in this study are limited to one office building, and generalized conclusions may require more case support.

6. Conclusion

This study demonstrates a Markov chain-based approach for rapid respiratory infection risk assessment in multi-zone buildings with relatively fixed occupants. The method combines real building information and occupant behavioral data to model time-dependent and time-independent behaviors of occupants at a low time cost. Four transmission routes are considered, especially for the fine-grained characterization of close contact. Compared to CFD-based models that only simulate airborne transmission in a single space with stationary occupants, the proposed model in this paper allows for the calculation of occupants' different activities in a multi-zone building as well as the multiple transmission routes involved. In contrast to pedestrian dynamics-based models, which generally consider only short-range exposures and simplify the infection probability as a function of physical distance and duration, the model proposed in this paper describes in detail the physical transport process of droplets in close contact and also accounts for long-range exposures. Specifically, the study focuses on close contact during the movement of people and achieves an accuracy of 0.1 m in the calculation of large droplet and short-range airborne transmission, marking about a 5-fold enhancement in accuracy compared to the grid-based descriptions (0.5 m) in most previous models based on pedestrian dynamics. A university office building was selected as a case study to validate and demonstrate the model, and the effects of three non-pharmacological interventions including spatial layout, ventilation, and occupant behavioral control were examined.

The results showed that in multi-zone office buildings with low occupant mobility, short-range airborne transmission dominated over aerosol transmission. Spatial design interventions reduced the indoor infection risk by up to 10 % in a 30-person office as a result of optimizing a combination of zone layout, furniture layout and facility layout. For the three types of spatial interventions, optimizing the zone layout was the most effective in reducing the infection risk, with Zone Layout A, which divides the open-plan office area into three subzones, reducing the risk by 9.6 %. Followed by the furniture layout, without changing the seating capacity and without desktop baffles, the L-shaped table layout worked better reducing the risk by 2.78 %. For the facility layout, the base scenario was more appropriate, on the contrary placing all the utilities in the main traffic area of the open office area increased the risk by 3.77 %. Furthermore, comparing the effects of spatial interventions with the effects of common interventions such as wearing masks and maintaining interpersonal distance showed that the intervention of zone layout was superior to the intervention of maintaining a one-meter interpersonal distance in such office environments. In addition, the proposed Zonal Cumulative Viral Exposure Dose (ZCVE) parameter can be used to characterize the level of zonal risk, where the larger the value, the more people in the zone are likely to be infected. Areas with high occupancy, complex activities, and more crossover between activity sites tend to have higher ZCVE values.

Analysis of the effects of spatial, behavioral, and ventilation interventions can help architects and managers better understand the risk of indoor transmission in multizone buildings from a spatial design perspective, as well as the relationship between the built environment and human health, in order to select appropriate interventions to reduce the risk. In addition, the model presented in this paper can be used to examine the risk of respiratory infections in multizone office buildings at the building level, not only at the room level, which is critical for the safe opening and use of public buildings. The model can be applied to other similar building types with relatively fixed occupants, such as inpatient buildings, by freely customizing the space configuration and occupant activity information.

CRediT authorship contribution statement

Qi Zhen: Writing – original draft, Investigation, Data curation, Conceptualization. **Anxiao Zhang:** Writing – review & editing, Supervision, Methodology, Funding acquisition, Conceptualization. **Regina Bokel:** Writing – review & editing, Supervision, Formal analysis. **Yue Zheng:** Investigation, Formal analysis. **Jing Li:** Resources, Investigation. **Yiming Du:** Validation, Investigation. **Qi Zhang:** Writing – review & editing, Supervision.

Declaration of competing interest

The authors declare that they have no known competing financial interests or personal relationships that could have appeared to influence the work reported in this paper.

Data availability

Data will be made available on request.

Acknowledgments

This research was supported by the 2023 Tianjin Philosophy and Social Science Planning Project (TJGLQN23-007), China.

References

[1] Yuguo Li, Cheng Pan, Wei Jia, Poor ventilation worsens short-range airborne transmission of respiratory infection, Indoor Air 32 (1) (2022) e12946.
[2] Qi Zhen, et al., Overview of the role of spatial factors in indoor SARS-CoV-2 transmission: a space-based framework for assessing the multi-route infection risk, Int. J. Environ. Res. Publ. Health 19 (17) (2022) 11007.
[3] Yunchen Bu, et al., Recent research on expiratory particles in respiratory viral infection and control strategies: a review, Sustain. Cities Soc. 73 (2021) 103106.
[4] Nan Zhang, et al., Close contact behavior in indoor environment and transmission of respiratory infection, Indoor Air 30 (4) (2020) 645–661.
[5] Zhiqiang Zhai, Facial mask: a necessity to beat COVID-19, Build. Environ. 175 (2020), 106827-106827.
[6] Yao Xiao, et al., Modeling indoor-level non-pharmaceutical interventions during the COVID-19 pandemic: a pedestrian dynamics-based microscopic simulation approach, Transport Pol. 109 (2021) 12–23.
[7] Nan Zhang, et al., Real human surface touch behavior based quantitative analysis on infection spread via fomite route in an office, Build. Environ. 191 (2021) 107578.
[8] Jeremy Michalek, Ruchi Choudhary, Panos Papalambros, Architectural layout design optimization, Eng. Optim. 34 (5) (2002) 461–484.
[9] Ziwei Cui, et al., Influences of obstacle factors on the transmission trends of respiratory infectious diseases in indoor public places, J. Build. Eng. 64 (2023) 105706.
[10] Anxiao Zhang, et al., Assessing the impact of architectural and behavioral interventions for controlling indoor COVID-19 infection risk: an agent-based approach, J. Build. Eng. 74 (2023) 106807.
[11] Neeltje Van Doremalen, et al., Aerosol and surface stability of SARS-CoV-2 as compared with SARS-CoV-1, N. Engl. J. Med. 382 (16) (2020) 1564–1567.
[12] Jennifer Biryukov, et al., Increasing temperature and relative humidity accelerates inactivation of SARS-CoV-2 on surfaces, mSphere 5 (4) (2020) 10–1128.
[13] C. Contardo, L. Costa, On the Optimal Layout of a Dining Room in the Era of COVID-19 Using Mathematical Optimization, arXiv, 2021.
[14] E. Ronchi, R. Lovreglio, EXPOSED: an occupant exposure model for confined spaces to retrofit crowd models during a pandemic, Saf. Sci. 130 (2020) 104834.
[15] Shubham Srivastava, et al., Effective ventilation and air disinfection system for reducing coronavirus disease 2019 (COVID-19) infection risk in office buildings, Sustain. Cities Soc. 75 (2021) 103408.
[16] Asmaa M. Hassan, Naglaa A. Megahed, COVID-19 and urban spaces: a new integrated CFD approach for public health opportunities, Build. Environ. 204 (2021) 108131.
[17] Xiangdong Li, et al., A spatiotemporally resolved infection risk model for airborne transmission of COVID-19 variants in indoor spaces, Sci. Total Environ. 812 (2022) 152592.
[18] Prateek Shrestha, et al., Multizonal modeling of SARS-CoV-2 aerosol dispersion in a virtual office building, Build. Environ. 206 (2021) 108347.
[19] Jiamin Guo, et al., Multizone modeling of pressure difference control analyses for an infectious disease hospital, Build. Environ. 206 (2021) 108341.
[20] W. Chen, N. Zhang, J. Wei, H.-L. Yen, Y. Li, Short-range airborne route dominates exposure of respiratory infection during close contact, Build. Environ. 176 (2020) 106859.
[21] Takemi Sugiyama, et al., Office spatial design attributes, sitting, and face-to-face interactions: systematic review and research agenda, Build. Environ. 187 (2021) 107426.
[22] Kerstin Sailer, Ian McCulloh, Social networks and spatial configuration—how office layouts drive social interaction, Soc. Network. 34 (1) (2012) 47–58.
[23] Erik Andresen, Mohcine Chraibi, Armin Seyfried, A representation of partial spatial knowledge: a cognitive map approach for evacuation simulations, Transp. A: Transp. Sci. 14 (5–6) (2018) 433–467.
[24] A. Gharaveis, D.K. Hamilton, D. Pati, The impact of environmental design on teamwork and communication in healthcare facilities: a systematic literature review, HERD: Health Environ. Res. Des. J. 11 (1) (2018) 119–137.
[25] S. Xiao, et al., Probable transmission routes of the influenza virus in a nosocomial outbreak, Epidemiol. Infect. 146 (9) (2018) 1114–1122.
[26] B. Hillier, J. Hanson, The Social Logic of Space, Cambridge university press., 1989.
[27] Sanmay Shelat, et al., A Markov-chain activity-based model for pedestrians in office buildings, in: Collective Dynamics, vol. 5, 2020, pp. 423–430.
[28] Chuang Wang, Da Yan, Yi Jiang, A novel approach for building occupancy simulation, in: Building Simulation, vol. 4, Tsinghua Press, 2011.
[29] Satu Sarjala, Built environment determinants of pedestrians' and bicyclists' route choices on commute trips: applying a new grid-based method for measuring the built environment along the route, J. Transport Geogr. 78 (2019) 56–69.
[30] Nick Davies, Who walks, where and why? Practitioners' observations and perspectives on recreational walkers at UK tourist destinations, Ann. Leis. Res. 21 (5) (2018) 553–574.
[31] Zhan Guo, Becky PY. Loo, Pedestrian environment and route choice: evidence from New York City and Hong Kong, J. Transport Geogr. 28 (2013) 124–136.
[32] Donald B. Johnson, A note on Dijkstra's shortest path algorithm, J. ACM 20 (3) (1973) 385–388.
[33] Christopher Yu Hang Chao, et al., Characterization of expiration air jets and droplet size distributions immediately at the mouth opening, J. Aerosol Sci. 40 (2) (2009) 122–133.
[34] Kai K. Lee, et al., Four-hour cough frequency monitoring in chronic cough, Chest 142 (5) (2012) 1237–1243.
[35] Wenzhao Chen, et al., Extended short-range airborne transmission of respiratory infections, J. Hazard Mater. 422 (2022) 126837.
[36] Jianjian Wei, Yuguo Li, Enhanced spread of expiratory droplets by turbulence in a cough jet, Build. Environ. 93 (2015) 86–96.
[37] Irving Langmuir, Katherine Blodgett, A Mathematical Investigation of Water Droplet Trajectories, No. 5418. Army Air Forces Headquarters, Air Technical Service Command, 1946.
[38] W.H. Walton, A. Woolcock, The suppression of airborn dust by water spray, in: E.G. Richardson (Ed.), Aerodynamic Capture of Particles, British Coal and Utilization Research Board (B.C.U.R.A.), Pergamon Press, 1960, pp. 129–153.
[39] V. Vuorinen, M. Aarnio, M. Alava, V. Alopaeus, N. Atanasova, M. Auvinen, N. Balasubramanian, H. Bordbar, P. Erästö, R. Grande, et al., Modelling aerosol transport and virus exposure with numerical simulations in relation to SARS-CoV-2 transmission by inhalation indoors, Saf. Sci. 130 (2020) 104866.
[40] G. Buonanno, L. Stabile, L. Morawska, Estimation of airborne viral emission: quanta emission rate of SARS-CoV-2 for infection risk assessment, Environ. Int. 141 (2020) 105794.
[41] X. Xie, Y. Li, A.T. Chwang, P.L. Ho, W.H. Seto, How far droplets can move in indoor environments–revisiting the Wells evaporation-falling curve, Indoor Air 17 (2007) 211–225.

[42] S. Liu, M. Koupriyanov, D. Paskaruk, G. Fediuk, Q. Chen, Investigation of airborne particle exposure in an office with mixing and displacement ventilation, Sustain. Cities Soc. 79 (2022 Apr) 103718.
[43] U. EPA, Exposure Factors Handbook 2011 Edition (Final), US Environmental Protection Agency, Washington, DC, 2011.
[44] Mark Nicas, Gang Sun, An integrated model of infection risk in a health-care environment, Risk Anal. 26 (4) (2006) 1085–1096.
[45] J.P. Duguid, The size and the duration of air-carriage of respiratory droplets and droplet-nuclei, Epidemiol. Infect. 44 (6) (1946) 471–479.
[46] W.C. Adams, Measurement of Breathing Rate and Volume in Routinely Performed Daily Activities, Final Report Contract A033–205, 1993.
[47] J. Montufar, J. Arango, M. Porter, et al., Pedestrians' normal walking speed and speed when crossing a street, Transport. Res. Rec. 2002 (1) (2007) 90–97.
[48] Toru Watanabe, et al., Development of a dose-response model for SARS coronavirus, Risk Anal.: Int. J. 30 (7) (2010) 1129–1138.
[49] Samy Rengasamy, et al., Filtration performance of FDA-cleared surgical masks, J. Int. Soc. Respir. Prot. 26 (3) (2009) 54.
[50] D.F. Johnson, et al., A quantitative assessment of the efficacy of surgical and N95 masks to filter influenza virus in patients with acute influenza infection, Clin. Infect. Dis. 49 (2) (2009) 275–277.
[51] S.A. Sattar, et al., Transfer of bacteria from fabrics to hands and other fabrics: development and application of a quantitative method using Staphylococcus aureus as a model, J. Appl. Microbiol. 90 (6) (2001) 962–970.
[52a] M. Wein, Quantifying the routes of transmission for pandemic influenza, Bull. Math. Biol. 70 (3) (2008) 820–867.
[52b] Mark Nicas, Daniel Best, A study quantifying the hand-to-face contact rate and its potential application to predicting respiratory tract infection, J. Occup. Environ. Hyg. 5 (6) (2008) 347–352.
[53] P. Dabisch, M. Schuit, A. Herzog, K. Beck, S. Wood, M. Krause, S. Ratnesar-Shumate, The influence of temperature, humidity, and simulated sunlight on the infectivity of SARS-CoV-2 in aerosols, Aerosol. Sci. Technol. 55 (2) (2021) 142–153.
[54] H.A. Aboubakr, T.A. Sharafeldin, S.M. Goyal, Stability of SARS-CoV-2 and other coronaviruses in the environment and on common touch surfaces and the influence of climatic conditions: a review, Transbound. Emerg. Dis. 68 (2) (2021) 296–312.
[55] Roman Wölfel, et al., Virological assessment of hospitalized patients with COVID-2019, Nature 581 (7809) (2020) 465–469.
[56] Yen Lee Angela Kwok, Jan Gralton, Mary-Louise McLaws, Face touching: a frequent habit that has implications for hand hygiene, Am. J. Infect. Control 43 (2) (2015) 112–114.
[57] Dan Fu, et al., Linear self-calibration method for camera, Opto-Electronic Eng. 35 (1) (2008) 71–75.
[58] J.S. Jia, X. Lu, Y. Yuan, G. Xu, J. Jia, N.A. Christakis, Population flow drives spatiotemporal distribution of COVID-19 in China, Nature 582 (7812) (2020) 389–394.
[59] C.F. Xiong, S.H. Hu, M.F. Yang, W.Y. Luo, L. Zhang, Mobile device data reveal the dynamics in a positive relationship between human mobility and COVID-19 infections, Proc. Natl. Acad. Sci. U. S. A. 117 (44) (2020) 27087–27089.
[60] Thomas Harweg, Daniel Bachmann, Frank Weichert, Agent-based simulation of pedestrian dynamics for exposure time estimation in epidemic risk assessment, J. Publ. Health (2021) 1–8.
[61] Bokyung Lee, et al., Designing a multi-agent occupant simulation system to support facility planning and analysis for covid-19, in: Designing Interactive Systems Conference 2021, 2021.
[62] Shuai Li, et al., Integrated environment-occupant-pathogen information modeling to assess and communicate room-level outbreak risks of infectious diseases, Build. Environ. 187 (2021) 107394.
[63] J.H. Zou, Q.C. Zhao, W. Yang, F.L. Wang, Occupancy detection in the office by analyzing surveillance videos and its application to building energy conservation, Energy Build. 152 (2017) 385–398.
[64] N. Zhang, B. Su, P.T. Chan, T. Miao, P. Wang, Y. Li, Infection spread and highresolution detection of close contact behaviors, Int. J. Environ. Res. Publ. Health 17 (4) (2020).
[65] Zhitao Zhong, et al., Camera-based occupant behavior trajectory capture and on-site assessment of spatio-temporal transmission risk of airborne virus in a university office building, Build. Environ. 243 (2023) 110670.
[66] Xueze Yang, et al., Analysis of SARS-CoV-2 transmission in airports based on real human close contact behaviors, J. Build. Eng. 82 (2024) 108299.
[67] D. Weissberg, J. Böni, S.K. Rampini, V. Kufner, M. Zaheri, P.W. Schreiber, I.A. Abela, M. Huber, H. Sax, A. Wolfensberger, Does respiratory co-infection facilitate dispersal of SARS-CoV-2? investigation of a super-spreading event in an open-space office, Antimicrob. Resist. Infect. Control 9 (2020) 191.
[68] Shin Young Park, et al., Coronavirus disease outbreak in call center, South Korea, Emerg. Infect. Dis. 26 (8) (2020) 1666.
[69] Caroline X. Gao, et al., Multi-route respiratory infection: when a transmission route may dominate, Sci. Total Environ. 752 (2021) 141856.
[70] Ihab Hasan Hatif, et al., Influence of office furniture on exposure risk to respiratory infection under mixing and displacement air distribution systems, Build. Environ. 239 (2023) 110292.
[71] Wei Jia, et al., Individual heterogeneity and airborne infection: effect of non-uniform air distribution, Build. Environ. 226 (2022) 109674.